

Team 59 Project Technical Report for the 2018 IREC

Oranos Polytechnique Montréal *

École Polytechnique de Montréal, 2500 chemin de Polytechnique, Montreal, QC, H3T 1J6, Canada

May 25, 2018

This technical report presents the design rationale and distinctive features of Oronos Polytechnique's 2018 prototype and first hybrid rocket of the team at the 2nd Spaceport America Cup, taking place in New Mexico from June 19 to 23. The sounding rocket is first introduced, then the different subsystems are explained in further detail. The appendix presents performance data, test report, risk assessment analysis, pre-launch checklists and complete engineering drawings.

Nomenclature

COTS	Commercial Off-The-Shelf
SRAD	Student Researched And Designed
IREC	Intercollegiate Rocket Engineering Competition
SA Cup	Spaceport America Cup
AGL	Above Ground Level
LCO	Launch Control Officer
ISP	Specific Impulse

I. Introduction

The 2018 10,000ft hybrid prototype (SRAD), nicknamed *Prometheus*, is the result of several years of work and is the first hybrid rocket to be launched by Oronos Polytechnique, a team from Polytechnique Montréal, an engineering school from Québec, Canada. This rocket is entirely designed and manufactured by students, apart from parachutes and oxidizer tank, and aims to reach an altitude of 10,000ft AGL. The following section will give a brief overview of every subsystems of the hybrid powered rocket. Then, the systems are described and the mission is outlined. Several appendices complete the information concerning the specifications and operation of the rocket.

II. System Architectures Overview

Prometheus is a hybrid engine powered rocket. Figure 1 presents a cutaway figure depicting the integrated launch vehicle configured for the mission. As the figure shows, the rocket is divided in four bays. The Booster Bay includes the oxidizer tank, oxidizer supply system, the main valve and the combustion chamber. The Avionics Bay includes the antennas for real-time telemetry and all the homemade avionics PCBs necessary to the control of the recovery and the engine. The Recovery Bay includes the parachutes, the shockcords and the two tender descenders. The Payload Bay is located in the nosecone and includes the payload, which is a block of steel for the first mission of *Prometheus*.

*Corresponding author: Olivier Jobin - Team Leader, olivier.jobin@oronospolytechnique.com

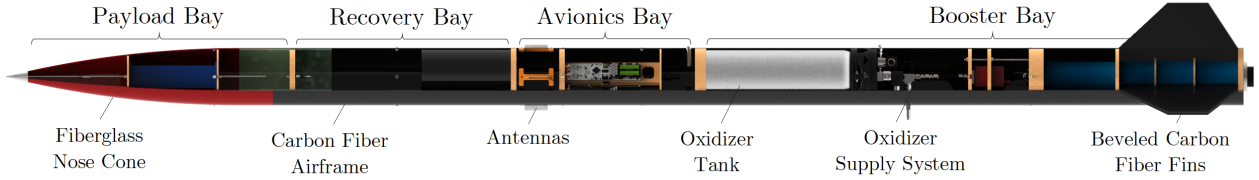


Figure 1: *Prometheus* integrated launch vehicle subsystems

II.A. Propulsion Subsystems

II.A.1. Oxidizer and Fuel Analysis

The first step the team had to make was to choose which oxidizer and fuel could provide good performance to propel the rocket to the desired altitude. Paraffin wax and Nitrous Oxide were chosen because this combination offers a variety of advantages, notably good performances, ease of acquirement and safety. The oxidizer's self-pressurized capacity also allows the simplification of the tubing required to route the oxidizer to the injector.

Paraffin wax is a mostly unreactive hydrocarbon, and this property is why it is simple to acquire. Its unreactive nature makes it difficult to release energy in a spontaneous or otherwise dangerous manner. It is therefore not considered too much of a safety hazard according to Canadian laws, and can be acquired easily by various means, such as online candle-making shops. This was a deciding factor in choosing this fuel, since Canadian laws restricting the use of more energetic and dangerous fuel make it difficult or impossible to obtain them. Other advantages to using paraffin wax include its fast regression rate compared to other solid hybrid fuels, and its easily modifiable properties through additives.

Some additives are used to enhance the performance of the paraffin, mainly the peak thrust, total impulse and Specific Impulse (ISP). The most notable one is an alpha-olefin, commonly called Vybar. Compared to pure paraffin, this additive effectively raises the melting point of the paraffin to keep its structural integrity in the high temperature of the desert and slows the regression rate to enhance the burn time. However, adding more Vybar seems to increase the regression rate, according to live engine tests done with 10%, 17.5% and 20%. In other words, any mixture of paraffin-Vybar has a lower regression rate than a pure paraffin one, but increasing the amount of Vybar results in an upwards trend related to the regression rate.

Another additive used is black candle dye. This additive does not directly affect the properties of the paraffin-Vybar mixture in a drastic way, but instead serves as an aid to the combustion process. The dye makes the fuel opaque to concentrate the radiation heat from the flame on the surface of the fuel port. This results in a decrease in combustion instabilities and unburned products.

Multiple tests were done to characterize the paraffin, with varying proportions of Vybar. Prior to the complete engine tests to verify live engine performance, advanced methods such as Differential Scanning Calorimetry (DSC) and rheometry were used to obtain insight on the combustion of the paraffin-Vybar mixture such as the melting points of each components of the fuel grains and the shear stress. The following samples were used in the tests, of which the graphs and analysis are available below:

Table 1: Sample Data

#Sample	Paraffin mass(g)	Vybar mass(g)	Total mass(g)	Paraffin % _m	Vybar % _m
1	25,19	5,038	30,228	83,33	16,67
2	25,19	2,519	27,709	90,91	9,09
3	26,58	1,329	27,909	95,24	4,76
4	27,63	0,691	28,321	97,56	2,44
5	25,81	0,323	26,133	98,76	1,24

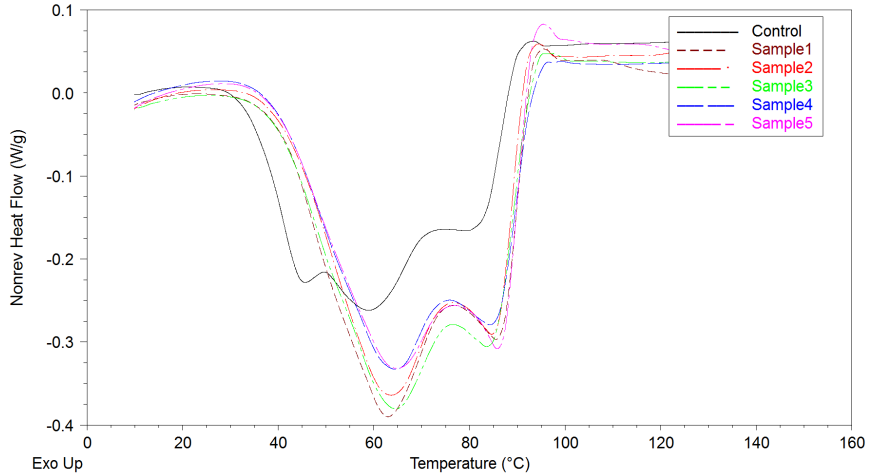


Figure 2: DSC tests, Heating phase

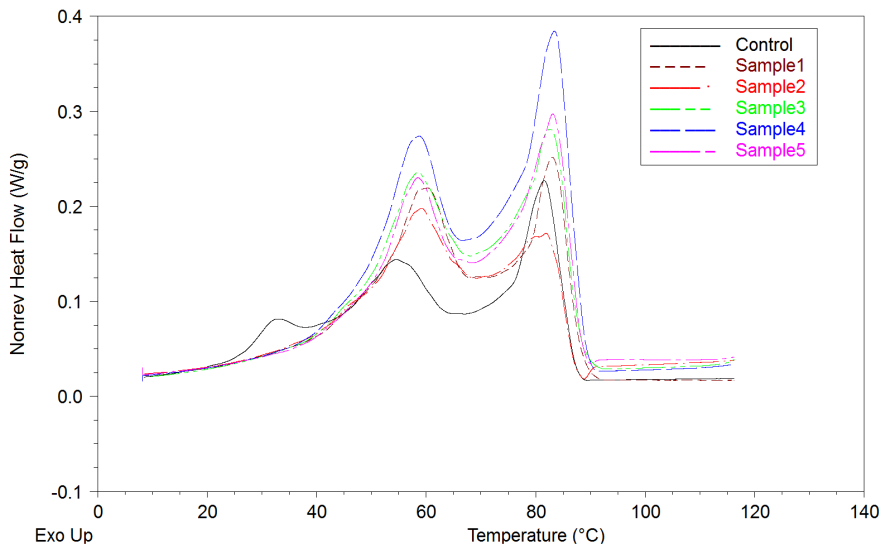


Figure 3: DSC tests, Cooling phase

With the control sample containing no Vybar, it is possible to see multiple properties of the paraffin-Vybar mixture in graph 2, which represents the heating phase. The asymmetric melting peak is an effect of having a mixture, while the double peaks mostly represent the melting point of each component, here clearly distinct from one another. In comparison with the control sample, the melting temperatures of all samples have increased. The exothermic nature of the reaction is seen as an increase in heat flow after the melting peaks, and as a small peak before the linear regime.

The cooling phase, seen in graph 3, is functionally the same graph, but reverse related to the heat flow. The two solidification peaks are again very distinct.

Below are the results of the rheology tests, using the same samples.

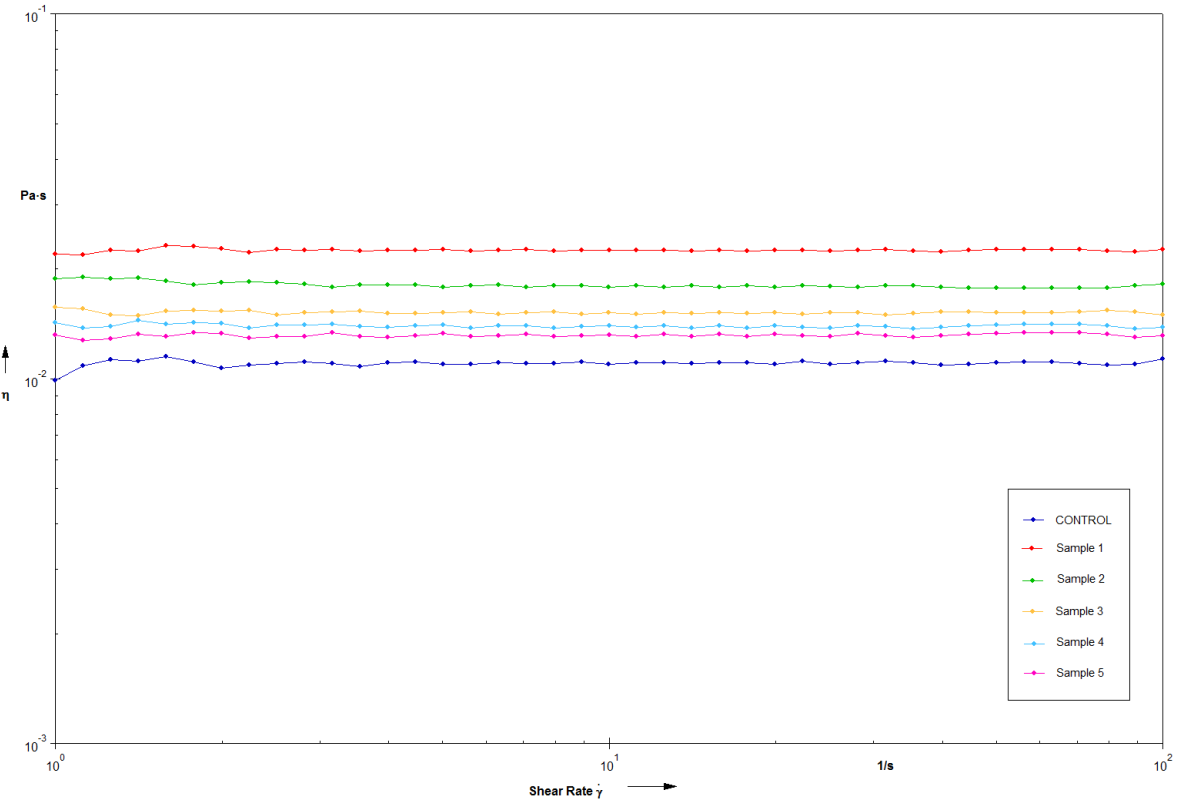


Figure 4: Rheometer tests

A coaxial cylinder geometry was used to achieve the rheology results seen in figure 4. The test was done at 100 °C to ensure complete liquification of the paraffin, according to the DSC results. The influence of Vybar on viscosity is very apparent. With the Vybar mass percentage decreasing as the sample number goes up, the result is a graph which clearly shows the increasing viscosity as more Vybar is added. The mechanical effects of Vybar on paraffin were then confirmed, and its properties could now be taken into account when choosing Vybar mass percentages for live engine tests. Indeed, as Vybar percentage increases, the fuel grains become more brittle, leading to various effects, both positive and negative.

A more brittle grain is more difficult to work with, since the manufacturing of the final dimensions has to take into account this brittleness in order to prevent breaking the grain. Once the grain has its final form, it can still be handled the same as most other non-reactive solid rocket fuels, meaning the brittleness isn't glass-like, but more like a semi-dry candle. The effects of brittleness are very important to take into account during combustion. A possible positive effect of brittleness is the breaking of the grain into very small crystals when combustion and viscous forces are applied to the port. This leads to an increase in surface area, generally meaning higher performance and combustion efficiency. However, if the crystals are too big, i.e. macroscopic chunks, they might not have time to completely burn up and will simply be ejected by the nozzle. This phenomenon is characterized by a decrease in combustion efficiency, increased nozzle strain and overall lower performance, since some matter is unburned. Some pressure peaks can also appear during the passing of these chunks through a nozzle, followed by pressure drops which affect performance.

II.A.2. Performance Analysis

Several static fires were done in order to characterize the motor's performance. While all tests had the goal of characterizing the engine performance and familiarize with the data acquisition system, some also had a more precise

objective.

Table 2: Static Fire Tests done on Hybrid Motor

Test	Date	Number of Burns	Objective	Notes
1	October 2016	2	Injector Design	Traditional and Swirl Injector burns
2	May 2017	1	Performance assessment	Successful burn; data acquisition problems
3	October 2017	1	Additive percentage effects	Premature valve shutdown
4	February 2018	1	Accurate Thrust Curve	Nozzle Malfunction; incomplete data
5	May 2018	1	Accurate Thrust Curve	TBD

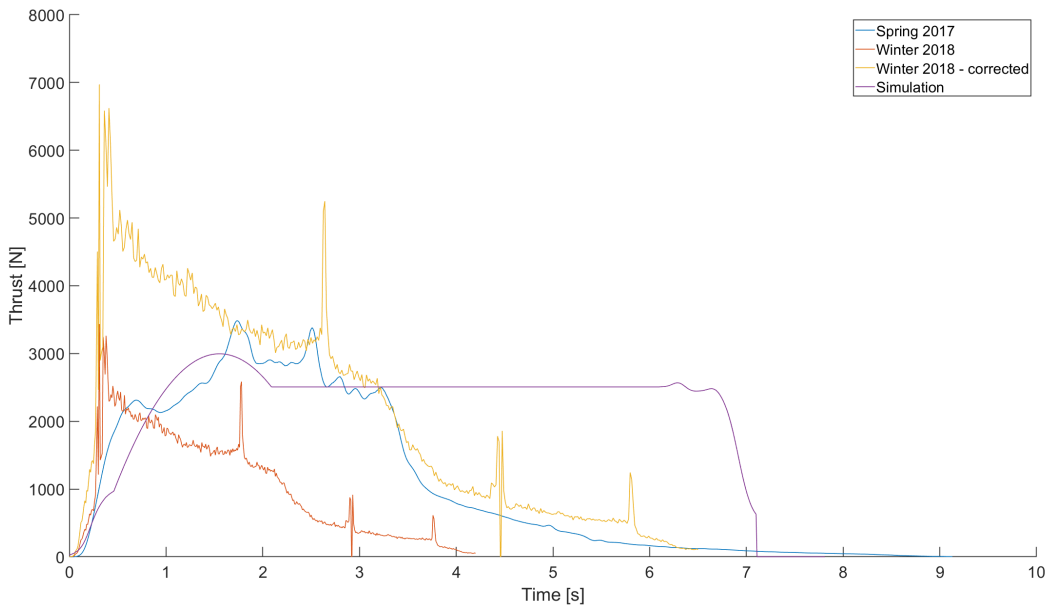


Figure 5: Important thrust data, various tests

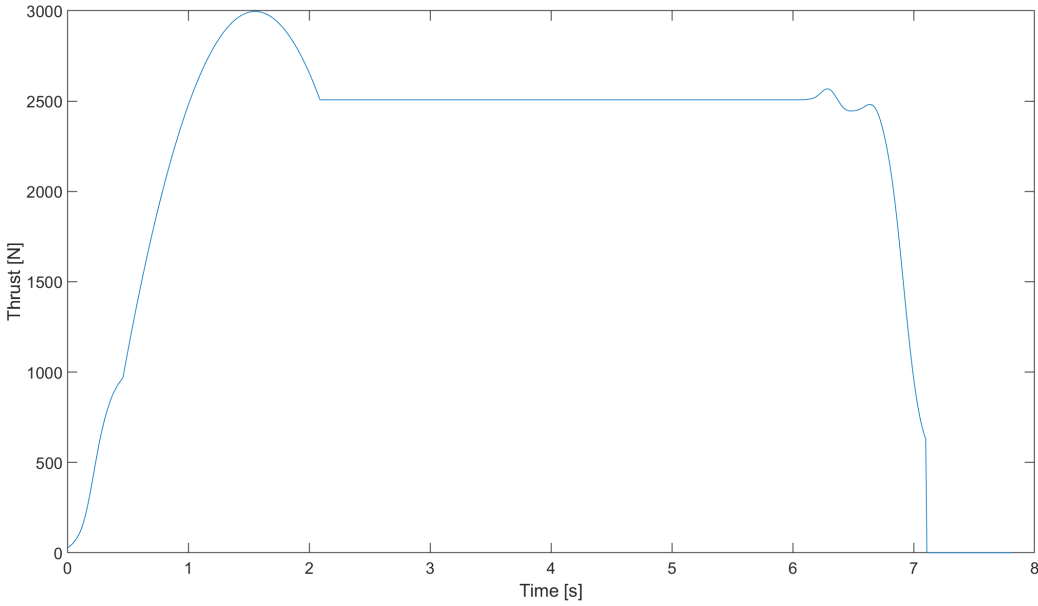


Figure 6: Thrust data used for flight simulations

The above figures display important thrust curves retrieved during tests which were done this year. Figure 5 shows all curves, for comparison purposes. Despite many successful burns, the thrust curve used to simulate flight characteristics is a theoretical one. Reasons for this are explained below, with the test analyses.

The Autumn 2017 test was subject to some problems which led to its performance being sub-par. First of all, the ambient temperature and previous oxidizer purge left the oxidizer tank cold, which meant a low pressure. The pressure was almost half what is expected in the competition's context. This leads to a much lower thrust, as per Sutton's¹ equations. This also led to the problem of the combustion chamber pressure being higher than the oxidizer tank pressure at times. This resulted in a reverse of flow, effectively halting oxidizer intake because of the installed non-return valve. Additionally, the intense vibrations generated by the burn created a disconnection in the avionics system, shutting the feed valve off due to a safety system. Analyses have shown that 51% of paraffin wax burned during this test, leading to the conclusion that the burn time would have been around twice the recorded burn time. This observation has been taken in consideration for the Winter 2018 corrected thrust curve. In summary, this test was useful as a whole to pinpoint design problems, and with these problems identified, the data could be used to continue optimization of the engine.

The Winter 2018 test was done in the middle of winter, but heat blankets protected the oxidizer tank from cold temperatures (around -10 °C), and a decent oxidizer pressure was obtained, being kept at around 25 °C and 800 Psi. A few tenths of a second after ignition, the nozzle broke off from the retainer ring attaching it to the aluminum casing. After further analysis, the nozzle failure was determined to be the result of fatigue from other hot fire tests, increased brittleness from the cold temperature and increased pressure from paraffin chunks passing through the nozzle neck. This nozzle-less burn seemed normal from afar, but the data showed thrust and burn time that were both lower than we expected. The data was then analyzed as an orifice plate system, which was deemed an acceptable approximation, since the retainer ring still acted as a choke. Some parameters such as combustion efficiency could still be retrieved. Using the previous tests' data for the missing parameters, a model using NASA's CEA tool could be adapted to our nozzle dimensions, resulting in the corrected Winter 2018 curve. It was determined that the total impulse would have been around 2.2 times higher than the recorded data.

Since a completely instrumented burn, with no valve or nozzle problems, is yet to be done, a simulated curve was made, mainly due to the lack of testing grounds. Using our test's data, and Sutton's¹ documentation, a mathematical model was built, mirroring what is to be expected of our engine, in the competition's context of pressure and temperature. A third degree polynomial curve is used to simulate the ignition, coupled with the non-instantaneous opening of

the oxide valve. The thrust peak amplitude and duration is determined according to our experimental data and NASA's CEA tool. The permanent regime is then a plateau, with a duration of approximately 5 seconds, which is expected according to regression rate and fuel volume. It is expected that the engine will possibly have shorter burn than this curve , but a higher thrust peak at ignition, both because of higher temperatures and pressures, resulting in similar total impulse. A test is scheduled before the competition, but it will possibly take place after this report has been submitted.

Results are presented in table 3.

Table 3: Results of various tests

Test	Total Impulse [Ns]	Avg. Thrust [N]	Isp [s]	Burn time [s]
Spring 2017	8128	2322	202	3.50
Autumn 2017	4227	1300	121	3.25
Winter 2018	4275	1016	70	4.20
Winter 2018 - corrected	13609	1979	137	6.50
Simulation	16473	2359	153	6.58

II.A.3. Ignition System

Ignition is done using a small, electrically-ignited K-class solid motor. This small motor's burn heats the paraffin, ensuring its combustion when the oxidizer is injected. The solid motor's ignition is electronically detected. Further details can be found in the avionics section of this report. The ignition sequence, which was successfully tested during static fires, is as follows:

1. Solid Motor ignition
2. Ignition detection
3. Oxidizer injection

II.A.4. Fluid Circuit System and Fueling architecture

Figure 7 shows a diagram of the rocket's oxidizer supply system. The oxidizer, in biphasic form, is pressurized by its vapor pressure : in the neighborhood of 850 psi at expected temperatures of 77 to 93 degrees F. The tubing is separated into two lines; one is connected to the liquid phase on the bottom of the tank, and the other to the gaseous phase, through a tube opening at 80% of its height.

The liquid phase section includes the infill, purge valve, and main valve. The purge valve's purpose is to quickly empty the rocket of oxidizer in case of emergency, without the rapid expulsion producing thrust as it would through the main valve and nozzle.

The main valve is connected with flexible tubing. This tubing's purpose is to perfit a radial offset of the valve, as its passage hole is not centered as seen from above. Without this offset, the valve would require a larger fuselage to fit into, which would heavily influence design in multiple areas. Rigid bent tubing was considered, but flexible tubing offers easier assembly and more flexibility in the exact position of the valve.

The gaseous phase section includes the bleed opening, which serves to control the proportion of phases in the tank. By venting gaseous oxidizer while liquid is being input, we can increase the proportion of liquid, to the required ratio of 4:1 liquid to gas. A pressure transducer is also included, to monitor oxidizer pressure.

The service pressure of the Luxfer commercial vessel tank is 2216 psi. All other components are from Swagelok and their service pressures are designed to be over the nominal pressure of 850 psi. All static fire tests used the in-flight components of the fluid circuit.

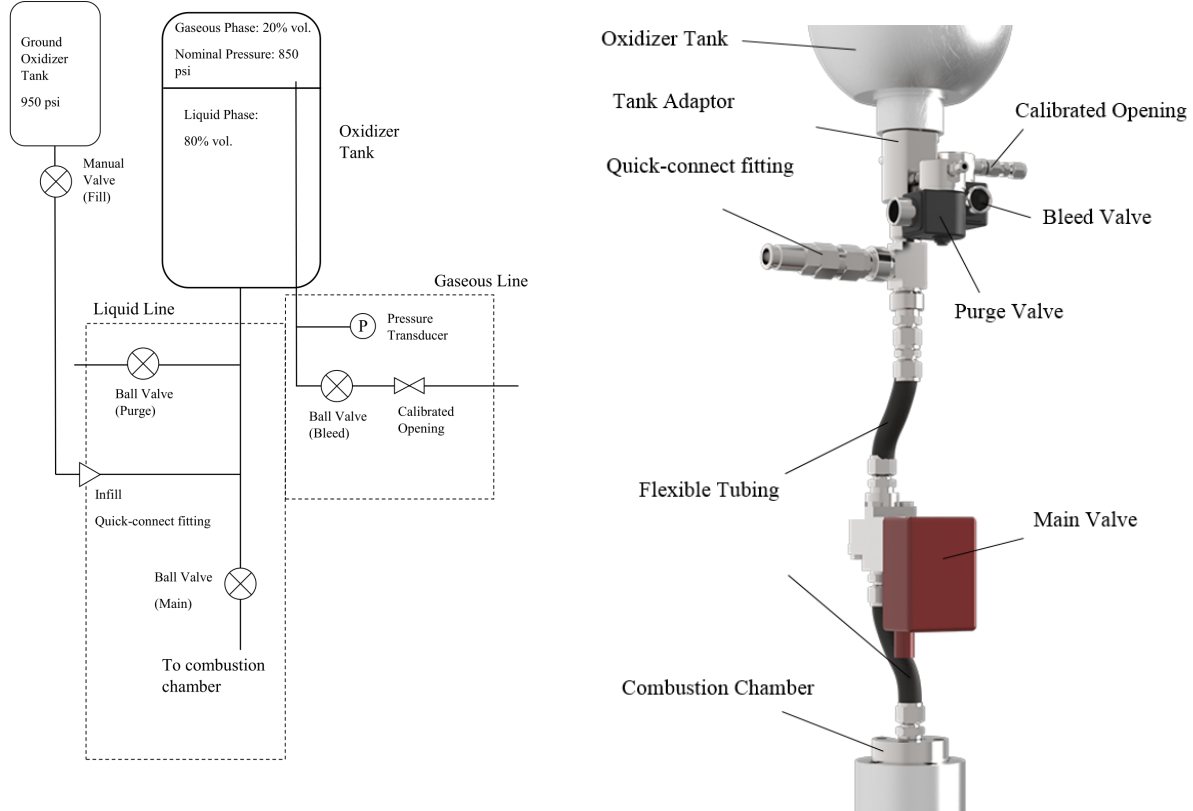


Figure 7: Oxidizer Supply System

II.A.5. Characterization and Analysis of a Swirl Injection

Many hybrid rocket engines suffer from low regression rate, particularly with this fuel/oxidizer combination. All other parameters equal, a lower regression rate implies a lower thrust; a minimum thrust is necessary to ensure stability. Studies have been made to increase this characteristic. A solution that one can apply is to use a swirling oxidizer injection system.

Using this type of injection system changes several parameters of the combustion. First of all, since the particles of nitrous oxide travel helicoidally within the combustion chamber, they will spend more time in a hot area. This will increase the temperature of combustion of the nitrous oxide and the paraffin wax, increasing performance. Secondly, the centrifugal effect caused by the rotation of the nitrous oxide will push the the fluid toward the wall of the combustion chamber. This will create an additional pressure component on the paraffin, resulting in an increased regression rate.

To test those interesting characteristics, a hot fire test was made to compare the effect of a traditional injector and a swirling injector. The motor tested was a smaller one that will propel *Prometheus*. The oxidizer, fuel components, oxidizer pressure and any other form factors were chosen in order to compare the results with the main engine. The results can be found in table 4.

Table 4: Results of hot fire test - Traditional injector vs. Swirling injector

	Traditional injector	Swirling injector	Gain (%)
Burn time [s]	2.95	3.53	+19.7
Total impulse [Ns]	899	1721	+91.4
Avg. Thrust [N]	305	487	+59.7

As it appears, the thrust and the total impulse were better with a swirling injector. The burn time is also slightly enhanced. The last parameter disagrees with the previous theory that a swirling injector improves the regression rate. However, when the combustion temperature tends to be higher, the paraffin wax will liquefy more, resulting in a more complete combustion. We observed that when the combustion is not efficient, chunks of paraffin wax were expelled from the combustion chamber and reduced the burn time.

II.B. Aero-Structures Subsystems

II.B.1. Structural design and analysis

The structure of the rocket consists of various composite material parts. Their role is to ensure that the vehicle has the necessary structural integrity to be able to complete its mission of bringing an 8.8-lbs payload to a 10,000 feet AGL altitude. The airframe can be separated in three sections for analysis: the nosecone, the fuselage and the fins.

Bruhn ² detailed a method for analysis of a rocket structure by calculating the axial load, the shear load and the moment at every station of the vehicle. Torsional stress was considered to be negligible compared to the other loads. Three scenarios were evaluated throughout the flight: the maximum acceleration, the maximum dynamic pressure and the maximum of the product of the dynamic pressure with the angle of attack. For each scenario and load type, the maximum loads were combined to obtain a more conservative value to evaluate structural integrity. Table 5 shows the combined loads used for the analysis.

Table 5: Combined loads for analysis

Load type	Load value
Axial [lb]	675
Shear [lb]	-10
Moment [lb·in]	0.3

Detailed analysis using these values showed that the engine section is experiencing critical load. Classical laminate theory was used to extract the stresses in each ply of the laminate. Base point of the analysis was the typical legacy Oronos laminate made with CYCOM 5320-1 carbon fiber pre-impregnated unidirectional tape and 8-harness satin (8HS), [8HS/0/90/0/90/0/8HS]. A security factor of 90.5, obtained via the Tsai-Wu criterion, can be applied to the Table 5 values before the first-ply-failure of the laminate. This critical value was observed on the two 90° plies. To reduce the analysis required, couplers were designed to be stiffer than the fuselages; their selected stackup is [8HS/0/90/0/90/0/90/0/8HS].

Although this security factor is quite high, which indicates the possibility of reducing the required number of plies, the analyzed stack-up was still selected, as its high security factor can account for the uncertainties in the manufacturing process and in the assessment of the aerodynamic forces.

Analysis showed that the nosecone does not experience severe loading during the flight. Thus, the main design criterion was to ensure the best aerodynamic capabilities. Fiberglass was selected as the stiffness of carbon fiber was not required. Although carbon fiber is much lighter than fiberglass, the manufacturing, cost and accessibility of the latter surpassed that advantage.

The fins' critical loading being aeroelastic, it is necessary to select a design that ensures a good safety margin to flutter. Theodorsen's³ empirical correlations were used to find the required parameters to have the flutter's critical speed over the predicted maximum speed achieved during flight. As the fins' cross-sectional dimensions were driven

by performance considerations, shear modulus and thickness were the main parameters to eliminate flutter. Full carbon fins were selected, as carbon fiber exhibits the highest stiffness in readily available materials. Selected design is a stack-up of 18 plies of CYCOM 5320-1 carbon fiber 8-harness satin, with a shear modulus of 5.585 GPa and a thickness of a quarter of an inch.

Characterization of the quality of the carbon fiber parts was conducted to evaluate the level of porosity in the parts. Cross-section micrographic analysis, visible in Figure 8, shows a low porosity level, which was the desired outcome, since it implies a higher resistance to stress.

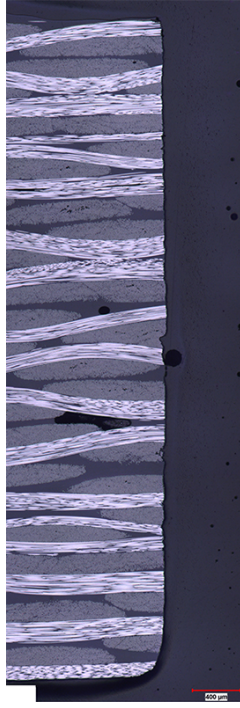


Figure 8: Micrograph of fins' cross-section

II.B.2. Stability and performance Analysis

To assess the stability and performance of the rocket, various simulations were performed. Here are the simulation steps presented from a design sequence point of view:

- An Excel worksheet with Barrowman's⁴ equations was used to provide basic aerodynamics coefficients and center of pressure position and explore the design space.
- An open-source rocket drag and stability simulator, Aerolab⁵, was used to validate the static analysis and explore the dynamic response and stability for the entire flight envelope. Special care is put to determine the static margin at take-off and max load conditions, which are the critical moments of the flight.
- Flight simulations were performed using two different sources (MATLAB in-house program and RASAero II⁶) and returned coherent results to reach the altitude of 10,000ft AGL. The simulation results for altitude, load factor and Mach number as a function of time are presented in Figure 9 to 11.
- Cambridge Rocketry Simulator⁷ was employed to characterize the three dimensional behavior to analyze the limitations and landing site probability with respect to typical wind conditions. This analysis is made to ensure that the landing site is within the boundaries of the expected recovery site and that the safety of the observers is guaranteed.

During the early phases of rocket design, its stability is of the highest priority, from a safety and a performance stand point. Fin design allows stable flight during the rocket's ascent, where the aerodynamic forces perpendicular to the axis of the rocket produce a moment to correct its flightpath. The center of gravity of the rocket was calculated

in advance (and corroborated experimentally as the construction progressed) based on the dimensions provided in the engineering drawings in Appendix 6.

The center of pressure, on the other hand, has been determined using the Barrowman method based on the aerodynamic characteristics and the dimensions of the rocket. The fidelity of the calculations was then extended with compressibility corrections using Aerolab.

The initial requirement imposed a stability margin above 1.5 from take-off to apogee. It was also necessary to make sure that the stability margin would stay under 6 for the whole duration of the flight so that the rocket would not be over-stable. This margin was evaluated in key events during the rocket's flight: at launch rail departure, at max Q, at motor burnout. In order to ensure optimal passive stability during the critical events of the rocket's flight, the moment created by the normal force coefficient ($C_n\alpha$) and the center of pressure (CP) was kept as close as possible to 70 during critical phases. The stability margin is estimated to be around 1.7 at liftoff. As opposed to a rocket flying with a solid motor, the variation (i.e. decrease) of the position of the center of gravity - due to the weight loss from the use of the propellant as the flight progresses - is not linear. This non linear variation is due to the fact that the center of gravity of the Nitrous Oxide drops during powered flight. Because our simulation softwares can only analyze flights for radial burning motors, it was necessary to perform a series of sensitivity analyzes of this center of gravity variation. The data gathered from these analyses, combined with the estimated center of pressure throughout the flight allowed for a simulation of the stability margin as a function of time to be made and the results are presented in Figure 12.

Drag is another important aerodynamic quantity of interest and it can greatly reduce the maximum altitude of a rocket. Knowing the fundamental aerodynamic properties of a rocket allows one to simulate its free flight, but the effects of different design choices are not always obvious. Estimating the drag of a model rocket is a rather complex task, and it involves numerically integrating the flight forces and determining the velocity, rotation and position of the rocket as a function of time. Aerolab was used as a simulation software as it outputs normal force coefficient, drag and stability margins, as well as a breakdown of the contributions of individual geometric components (nosecone, fins, etc.).

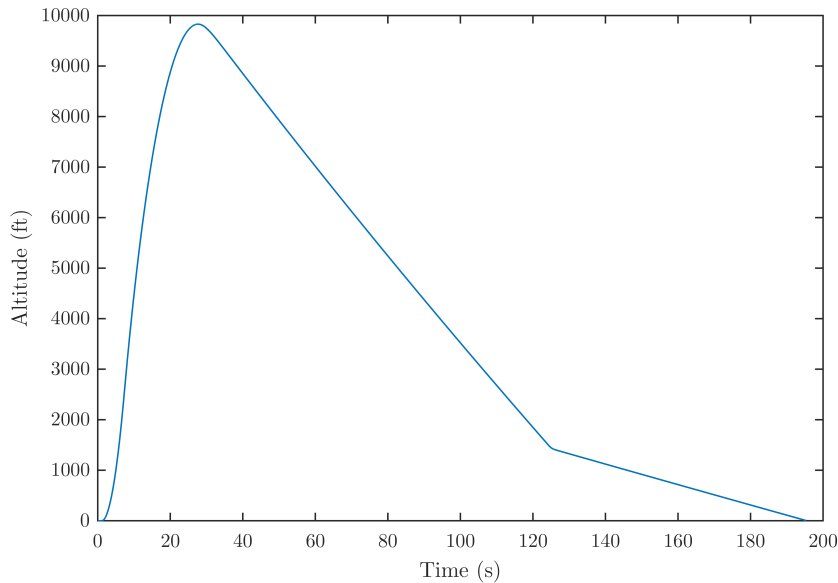


Figure 9: Simulated Altitude vs Time

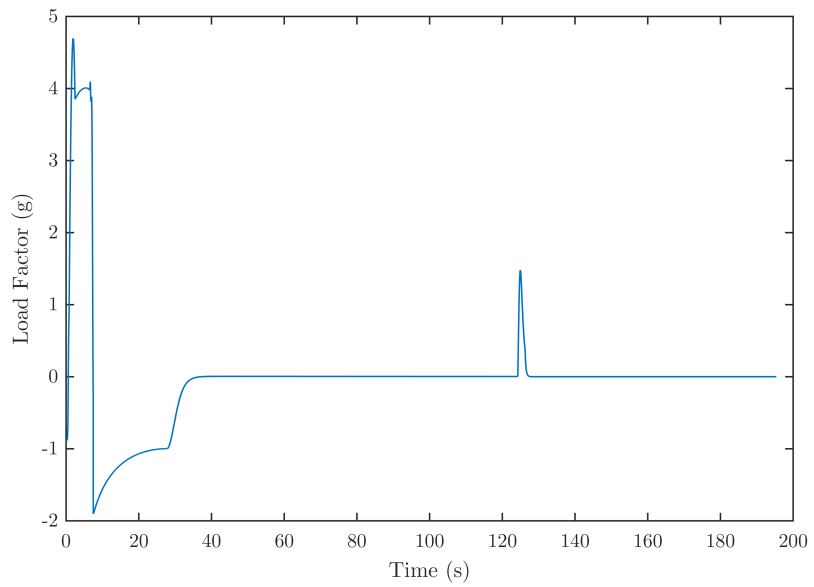


Figure 10: Load Factor vs Time

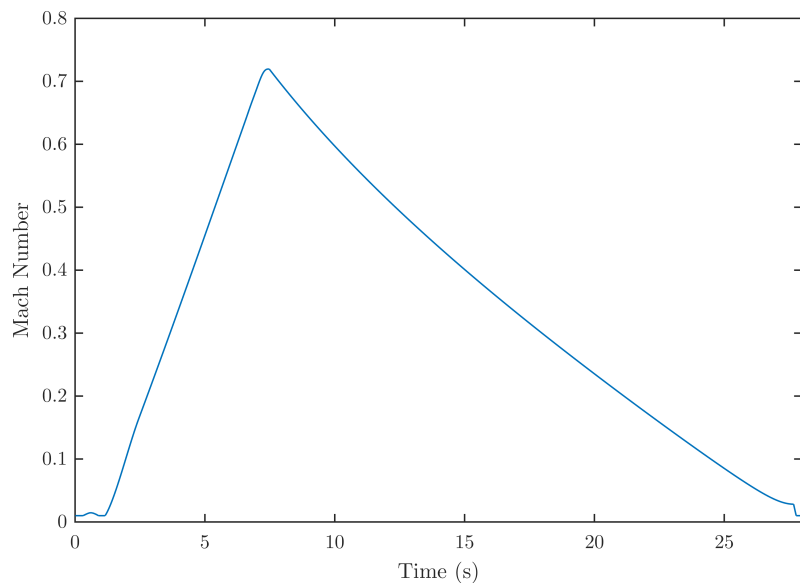


Figure 11: Mach Number vs Time

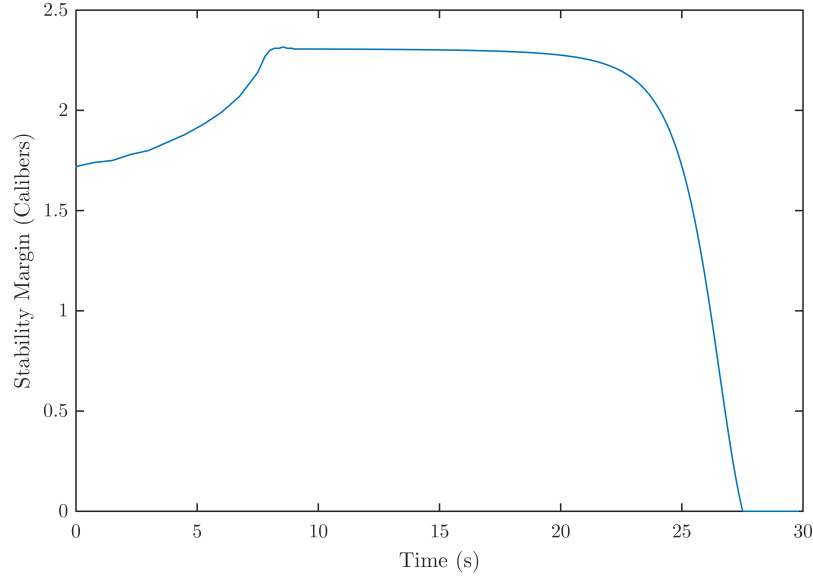


Figure 12: Stability Margin vs Time

The effect of wind on the flight of a rocket is often significant, especially for the descent phase. Usually, a stable rocket will point in the direction of the wind during ascent and get carried downstream for the rest of the flight. To estimate the landing position of the rocket, 6 degrees of freedom simulations were performed using the Cambridge Rocketry Simulator. The inputs were the same as for the other flight simulator: geometry, motor, and mass, with the addition of a prescribed atmosphere including wind. The weather on launch day was approximated based on the last 3 years publicly available data at Elephant Butte. Overall, the wind does not exceed 10mph, except for a few days where gusts up to 40 mph were present. Also, the wind direction is 270deg in the morning, and shifts to about 110deg in the afternoon. These inputs, combined with a 50 run Monte-Carlo simulation, gave the results presented in Figure 13. This landing site is on average about 1,650ft north and 1,750ft west of the launch site, which is acceptable and within the boundaries of the expected recovery site at Spaceport America Cup.

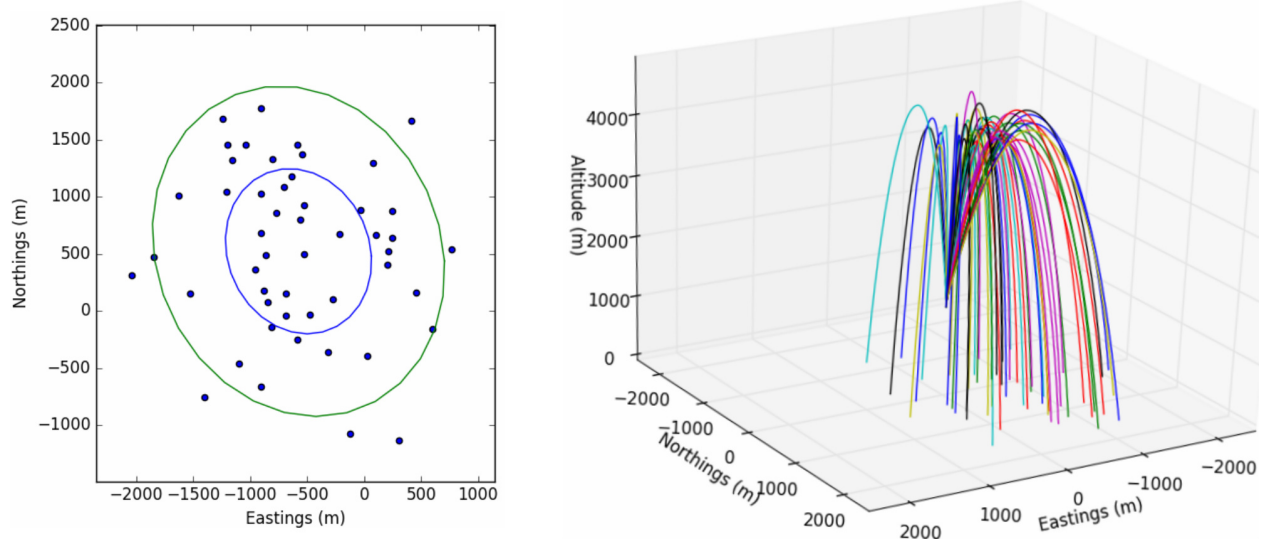


Figure 13: Landing Site Position

II.C. Recovery Subsystems

The recovery system consists of one separation and two parachute deployments (single separation, dual event).

The parachute bay is just above the avionics bay and they are separated by a bulkhead. Two ejection canisters (two for redundancy) made from PVC are glued with epoxy onto this bulkhead. The explosive charges are made of black powder and they are activated by overheating resistors (bridge wires) that are connected to wires. The wires go through the bulkhead and enter the canisters from the parachute bay and not from the avionics bay so the team can assemble and insert the avionics into the rocket the day before launch allowing fast and easy launch-day operations.

During the first event, the 36 inches drogue parachute will be deployed. The main parachute is held in the rocket by two tender descenders for redundancy. During the second event, the tender descenders let go and the 144 inches main parachute is deployed. These specific parachute sizes were chosen to ensure that the rocket's descent velocity respects the competition's requirements.

II.D. Avionics

The design team favored a light and compact avionics system to reduce the rocket's mass. The system is in the middle section of the rocket, which allows an easier access for the wiring to the parachutes and the engine. The avionics bay is mounted on a wood structure that has been optimized to be light, sturdy and easy to be installed in the fuselage. Figure 14 presents the avionics mounted on the wood structure.



Figure 14: Realistic 3D rendering of the avionics on the wooden structure

II.D.1. Architecture

The avionics module features five PCBs that are mounted on the wooden structure. The two Module for Control and Deployment V7 (MCDv7) and the Hybrid Avionics Module (HAM) are self-powered, and two COTS deployment modules (StratoLoggers) are powered by separate 9V batteries.

Each MCDv7 can perform most of the tasks of the mainline avionics bay. They deploy the parachutes, establish a radio link to the ground, log data, track the GPS position and monitor various statuses of the rocket. Both MCDv7 are networked via a fully redundant Controller Area Network (CANBus/ARINC 825) that has a maximum data rate of 2 Mbit/s (1 Mbit/s per bus). The protocol layer includes error detection and signaling. All modules can communicate directly with each other using the CANBus.

The HAM monitors thermal and pressure sensors and controls actuators that are in the engine section. It is also connected to the MCDv7 via CANBus, allowing it to send and receive data over radio. The HAM can perform a launch autonomously by detecting the presence of a flame in the rocket engine. The autonomous launch has a redundant algorithm to detect a fire in the rocket engine by reading the temperature and the continuity of four thermistors located in

the engine. This feature removes the need for a visual confirmation of the solid grain's ignition while also preventing oxidizer injection in the case of a misfire. There is also an arming sequence to prevent a false positive launch trigger. The HAM also can also control the oxidizer tank's bleeding and purge valves. For safety reasons, the HAM also implements a watchdog that will automatically purge the oxidizer if it loses contact with the Groundstation for more than 15 minutes.

An external multi-position switch allows each StratoLogger to be powered on individually, facilitating sound-based diagnostics. When the switch is on the "off" position, the StratoLogger's e-matches are also shunted to avoid static electricity hazards. The switch also allows the avionics bay to be turned on only once the rocket is on the launch pad. This allows the team to manipulate recovery charges while all electronic systems are unpowered.

II.D.2. Power and Radio Systems

Each MCDv7 has up to six hours of autonomy. The HAM is powered by four cylindrical cells to provide enough power to control the actuators and monitor the sensors. This board has up to 4 hours of autonomy including two full refueling sequence. The cells are easily accessible on either PCB if they need to be replaced. Both modules have an external charging port, allowing the batteries to be recharged even after the avionics bay has been assembled.

The radio system uses the 902-928 ISM band to provide a constant uplink and downlink to and from the rocket. Oronos uses custom made, inverted-F antennas, tuned at 915 MHz. Their form resembles a fin and they are mounted outside the rocket, near the avionics bay. Analysis of the impedance of the antennas shows results close to the ideal ($50 + j0$) ohms when a small strip of copper is placed on both sides of the antennas to prevent RF absorption from the carbon fiber and improve matching. A range of at least 5 miles is expected.

Since telemetry is essential to the takeoff sequence of the rocket, each MCDv7 provides a full-duplex communication link with the ground with minimal loss of data. The telemetry link acts as a virtual CANBus that links the ground PCBs and the Groundstation, allowing for control commands to be sent to the rocket.

II.D.3. Features

- Module for Control and Deployment, v7 (MCDv7)
 - Dual barometric pressure sensor with a resolution of 20 cm
 - Allows troubleshooting of any sensor malfunction through a robust voting algorithm
 - Reports igniter denotations
 - Remotely armed via radio connection
 - Detects separation and measures sink rate
 - Dual 915 MHz radio/antenna operating in full-duplex with the ground systems
 - Maximum bitrate of 500 kbits/s
 - GPS receiver
 - One 3D high-resolution accelerometer/gyroscope
 - Provides a 45V supply stored in capacitor bank to release the energy necessary to trigger the parachute deployment mechanism.
 - Provides live feedback of rockets altitude, position and inertial reference to the ground station
 - Data logging capabilities at a rate of 1 MByte/s on a MicroSD card
 - Sends instantaneous current usage information
 - Holds two high capacity lithium-ion cells
 - Charges the cells when plugged to an external power source
 - Features reverse voltage protection and fused circuits
 - Turned ON by a physical switch on the fuselage
 - Covered by a thin layer of conformal coating that protects from moisture, corrosion, thermal shock, and static discharges

- Hybrid Avionics Module (HAM)
 - Converts battery voltage to 3V/5V/24V used by the other subsystems
 - Controls up to four actuators
 - Monitors thermal and pressure sensors
 - Offers extra analog and digital input/output if required
 - Data logging capabilities at a rate of 1 Mbyte/s on a MicroSD card
 - Sends instantaneous current usage information
 - Holds four high capacity lithium-ion cells
 - Charges the cells when plugged to an external power source
 - Features reverse voltage protection and fused circuits
 - Turned ON by a physical switch on the fuselage
 - Covered by a thin layer of conformal coating that protects from moisture, corrosion, thermal shock, and static discharges

The recovery system is completely redundant. It includes two StratoLoggers and two MCDv7s, each of which can deploy the parachutes independently. The MCDv7s each use two different barometers for altitude calculation and share their data via the CAN bus, allowing for a robust voting algorithm that can detect and correct sensor failure. As long as at least one of the four barometers works properly, successful and still observe a successful recovery sequence by all PCBs. As an additional redundancy, two independently powered commercial Stratologgers can each deploy the parachutes.

- COTS Stratologger
 - Barometric pressure sensor
 - Reports e-match detonations with beeps
 - Gives official altitude
 - Turned ON by a physical switch on the fuselage
 - Shunted when the power switch is in the off position
 - Independently powered with a standard 9V battery

II.D.4. Launch sequence

When the rocket is completely ready to launch, the auto-launch-detect mode is enabled. When activated, the HAM will continuously poll four thermistors located in the combustion chamber until one of two events occur:

- The temperature detected by at least two of the thermistors exceeds a threshold or,
- The difference in temperature in the last forty measurements of at least two thermistors exceeds a threshold.

Once an event occurs, the main valve opens allowing the oxidizer to flow in the combustion chamber and launching the rocket. In other words, once the auto-launch-detect mode is enabled, the LCO can trigger the launch, which will ignite the solid rocket motor. The sudden temperature change in the combustion chamber will cause an event to be detected and the rocket will launch.

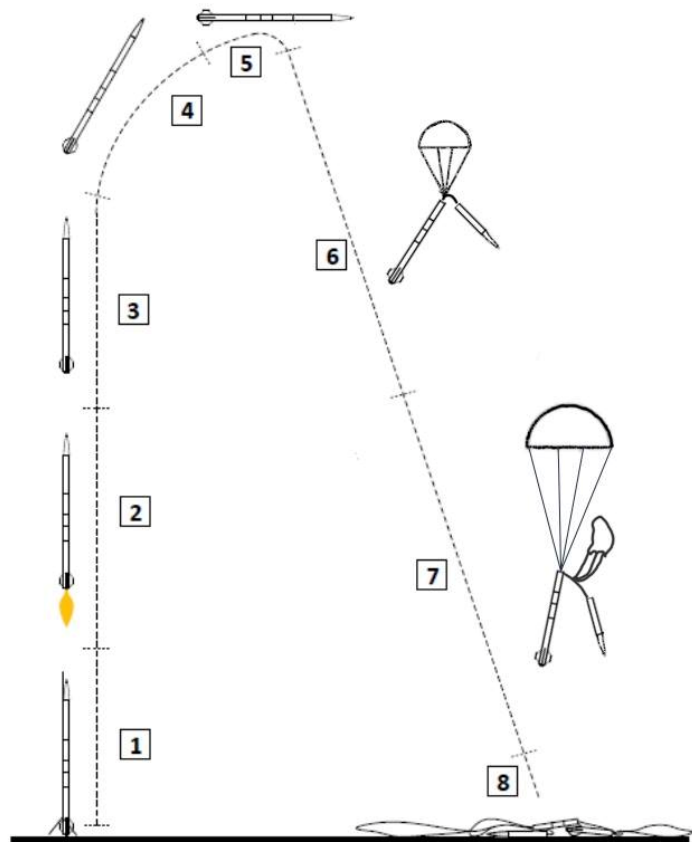
II.E. Payload Subsystems

To reduce complexity, a 4kg steel block is used as the payload. It has the form factor of a 3U CubeSat, which could be replaced by an actual CubeSat on future flights of this rocket.

III. Mission Concepts of Operations Overview

The aim of this section is to go through the phases of flight in order to establish the mission profile and nominal operations of the systems during each phase. Figure 15 shows a typical single-deployment rocket flight with numbers corresponding to each phase :

1. Rocket on launch ramp
2. Powered flight
3. Ballistic flight
4. Coasting phase
5. Apogee
6. Drogue chute descent
7. Main chute descent
8. Landing



Typical mission profile for single stage rockets. 1: Rocket on launch ramp.
2: Powered flight. 3: Ballistic flight. 4: Coasting phase. 5: Apogee. 6: Drogue chute descent. 7: Main chute descent. 8: Landing.

Figure 15: Rocket Flight Phases

Phase 1 consists of the rocket on the launch pad, just prior to launch. At this phase, the team has completed 2 checklists (assembly and pre-flight), reviewed all subsystems to make sure they are operational and assembly went smoothly, radio communication is clear and avionics are powered. Nominally, the launch procedures will be coordinated by a Launch Control Officer (LCO) and all unnecessary personnel has evacuated the launch site and only

essential people remain at the launch control facility. The LCO proceeds with the countdown and if any mishap occurs (hangfire, explosion, etc,), the team should refer to the launch checklist in Appendix 5. This phase ends with the correct ignition of the motor and liftoff of the rocket.

Phase 2 is the powered flight of the rocket. This is where the structural integrity and stability are of utmost importance and the Risk Assessment appendix addresses those issues. If the flight is nominal, the rocket should remain intact and continue its course in a straight line with some, but not excessive, roll. During this phase, the avionics acquire data and should detect only a decrease of ambient pressure and acceleration. This phase will last approximately for 7 seconds, which is the burn time of the rocket engine.

Phase 3 and 4 represent the majority of the ascent of the rocket. The figure distinguishes the two for the simple reason that the spectators will be able to tell when the rocket starts to rotate and coast. Nevertheless, these two phases are the same from the point of view of the systems and will be treated as such. The total time to apogee of *Prometheus* is 27 seconds, therefore the coasting phase will last 20 seconds. The rocket will slowly lose velocity until it reaches the apogee, which marks the end of this phase. At this point, the center of gravity is at its foremost and the rocket should not be overstable. The loads on the airframe are expected to be less than during the previous phase, but the load has shifted from being positive to negative (the rocket decelerates) and structural integrity and stability are still very important. The avionics should perform the same way as the last phase, without prematurely deploying the parachutes. In case of a structural failure or loss of control of the rocket, the LCO will announce to all spectators to get out of their tents and look at the vehicle (called a *Heads up!*). This is standard procedure at rocket launches.

Phase 5 constitutes the apogee of the rocket. It is formally defined as the time the rocket reaches the maximum altitude with respect to ground level. The nominal operation of the avionics during this phase is to register a rising ambient pressure, which indicates the rocket has started to fall back to earth, and trigger the pyrotechnics. Multiple modules will perform this task in parallel, for redundancy purposes. The fuselage section containing the drogue will break the shear pins and separate due to the increased pressure in the rocket. At this time, the 36in drogue parachute will deploy to slow down the rocket's descent to a velocity of 100ft/s. In real time, the radio link will still receive the flight data and crew on the ground will be able to determine whether the rocket has been slowed down (indicating correct deployment) or not. This phase, although it's one of the shortest, is the most critical. Several items of the Risk Assessment appendix treat potential malfunctions during this phase, including parachute deployment and structural integrity of the fuselages, shock cords and other recovery devices.

Phase 6 is the drogue chute descent of the prototype which starts when the drogue has successfully deployed. The avionics will continue to acquire data, although the apogee has been detected and the maximum altitude has been determined by both custom and commercial altimeters. Because of wind, the rocket usually spins and this may cause a risk that the eyenut linking the parachute to the sections detaches. This event is the most likely malfunction during the descent phase and is discussed in Appendix 4.

Phase 7 represents the main chute descent. This phase starts when the main parachute is deployed by the avionics. The criterion that triggers this event is a predetermined altitude of 1,500ft. When the avionics detects that it has reached this altitude relative to the launch site after a successful launch attempt, it sends a signal to trigger the pyrotechnics related to the main parachute. At this time, the 144in main parachute will deploy to slow down the rocket's descent to a velocity of 20ft/s. The same structural integrity risks that were at apogee are also true here. In case of event failure, the rocket will continue to descend under the drogue and poses a potential threat to spectators. Again, the *Heads up!* signal should be given if this happens.

Phase 8 is the landing of the rocket. The rocket poses no active threat at this point, except that unburnt pyrotechnics could still be live or the rocket engine may be still hot. The avionics is equipped with a timer that automatically deactivates after 10 minutes. It is important that the recovery team handles the prototype with care and respects this delay. Another important risk is if the recovery team underestimates the dangers associated with dehydration and sun exposure, but those are not related to the vehicle.

IV. Conclusions and Lessons Learned

This technical report detailed the design and specifications of the systems that constitute this year's hybrid SRAD 10k rocket. The Mission Concept of Operations Overview provided a full overview of the rocket's flight and discussed risks and nominal operation of all systems.

The Appendixes provide complementary information on the specifications (Appendix 1 Weights and Appendix 6 Engineering Drawings) and the operations of the rocket (Appendix 2 Test Report, Appendix 3 and 4 Risk Assessment, and Appendix 5 Checklists).

The conception of *Prometheus* was a 5 year project. Since the original members have all graduated, the transfer of knowledge has been a big challenge. Around 10 Preliminary Design Reviews and Critical Design Reviews were made throughout the project. All the different tests and critical decisions were put on paper to keep track of them. Those are the major techniques Oronos uses and will continue to use in order to improve and continue the optimization of this hybrid rocket.

As a team, we learned how to use highly complex systems and how to handle them professionally to reduce risks. We learned that engine testing is a critical part of the project, and it is not easily done. Having all the required documents and authorizations can be quite hard. Each engine test was prepared months in advance. The integration of the engine was also a great challenge. It is very different from all the other COTS engines that Oronos has used. The avionics also need to be modified to include the control of the hybrid motor.

Depending on this year's competition results, further improvements will be done on this rocket. Future projects could include a custom-made oxidizer tank, enhancement of combustion performances, by adding other additives, and finally the upgrading and/or upscaling of the rocket to create a version that could fly up to 30,000 ft.

V. Appendix 1: System Weights, Measures and Performance Data

THIS PAGE INTENTIONALLY LEFT BLANK



Spaceport America Cup

Intercollegiate Rocket Engineering Competition

Entry Form & Progress Update



Color Key

SRAD = Student Researched and Designed

v18.1

Must be completed accurately at all time. These fields mostly pertain to team identifying information and the highest-level technical information.

Should always be completed "to the team's best knowledge", but is expected to vary with increasing accuracy / fidelity throughout the project.

May not be known until later in the project but should be completed ASAP, and must be completed accurately in the final progress report.

Date Submitted: **2018-05-24**Country: **Canada**Team ID: **59** * You will receive your Team ID after you submit your 1st project entry form.State or Province: **Quebec**

State or Province is for US and Canada

Team InformationRocket/Project Name: **Prometheus**Student Organization Name **Oronos Polytechnique**College or University Name: **Polytechnique Montreal**Preferred Informal Name: **Optional**Organization Type: **Club/Group**Project Start Date **2017-09-01**

Projects are not limited on how many years they take

Category: **10k – SRAD – Hybrid/Liquid & Other**

Member	Name	Email	Phone
Student Lead	Olivier Jobin	olivier.jobin@oronospolytechnique.com	14384927110
Alt. Student Lead	Pablo Ponce Julien	ponce.pablo@outlook.com	14383995199
Faculty Advisor	Eduardo Olivera	eduardo.olivera@polymtl.ca	15142093794
Alt. Faculty Adviser			

For Mailing Awards:

Payable To:	Oronos Polytechnique
Address Line 1:	Polytechnique Montreal
Address Line 2:	2500, chemin Polytechnique (Porte S-114)
Address Line 3:	Montreal, Quebec
Address Line 4:	H3T 1J4
Address Line 5:	

Demographic Data

This is all members working with your project including those not attending the event. This will help ESRA and Spaceport America promote the event and get more sponsorships and grants to help the teams and improve the event.

Number of team members

High School	0
Undergrad	30
Masters	1
PhD	0

Male	27
Female	4
Veterans	0
NAR or Tripoli	1 (CAR)

Just a reminder the you are not required to have a NAR, Tripoli member on your team. If your country has an equivalent organization to NAR or Tripoli, you can count them in the NAR or Tripoli box. CAR from Canada is an example.

STEM Outreach Events

n/a

Rocket Information

Overall rocket parameters:

	Measurement	Additional Comments (Optional)
Airframe Length (inches):	166.75	
Airframe Diameter (inches):	7.71	
Fin-span (inches):	6	
Vehicle weight (pounds):	91.55	
Propellant weight (pounds):	24.25	
Payload weight (pounds):	8.8	
Liftoff weight (pounds):	124.6	
Number of stages:	1	
Strap-on Booster Cluster:	No	
Propulsion Type:	Hybrid	
Propulsion Manufacturer:	Student-built	
Kinetic Energy Dart:	No	

Propulsion Systems: (Stage: Manufacturer, Motor, Letter Class, Total Impulse)

1st stage : custom engine, hybrid ,N2O/paraffin, N,16500 (Ns)

Total Impulse of all Motors: 16500 (Ns)

Predicted Flight Data and Analysis

The following stats should be calculated using rocket trajectory software or by hand.

Pro Tip: Reference the Barrowman Equations, know what they are, and know how to use them.

	Measurement	Additional Comments (Optional)
Launch Rail:	Team-Provided	
Rail Length (feet):	20	
Liftoff Thrust-Weight Ratio:	5.5	
Launch Rail Departure Velocity (feet/second):	71	
Minimum Static Margin During Boost:	1.7	*Between rail departure and burnout
Maximum Acceleration (G):	4.7	
Maximum Velocity (feet/second):	796	
Target Apogee (feet AGL):	10K	
Predicted Apogee (feet AGL):	9830	

Payload Information

Payload Description:

a 10x10x30cm steel block will be installed as payload. Due to an already high cost for this rocket, it was deemed safer to reduce the risk of losing more expensive equipment in the event of a malfunction.

Recovery Information

For the hybrid rocket, the recovery system will be done with one separation and two parachute deployments (single separation, dual deployment).

The parachute bay is just above the avionic bay and they are separated by a bulkhead. Two ejection canisters made from PVC are glued with epoxy onto this bulkhead for redundancy. The explosive charges are made of black powder and they are activated by overheating resistors (bridge wires) that are connected to wires. The wires go through the bulkhead and enter the canisters from the parachute bay and not from the avionic bay so we can assemble and insert the avionic in the rocket the day before.

At the first event, the 36 inch drogue parachute will be deployed. The main parachute is held in the rocket by two tender descenders for redundancy. At the second event, the tender descenders let go and the 144 inches main parachute is deployed.

Planned Tests

* Please keep brief

Any other pertinent information:

Please help us to help you, by filling this box out as completely as possible. The more information we have the better we can help you.

(Tip: [Alt] + [Enter] for new line)

End of File

VI. Appendix 2: Project Test Reports

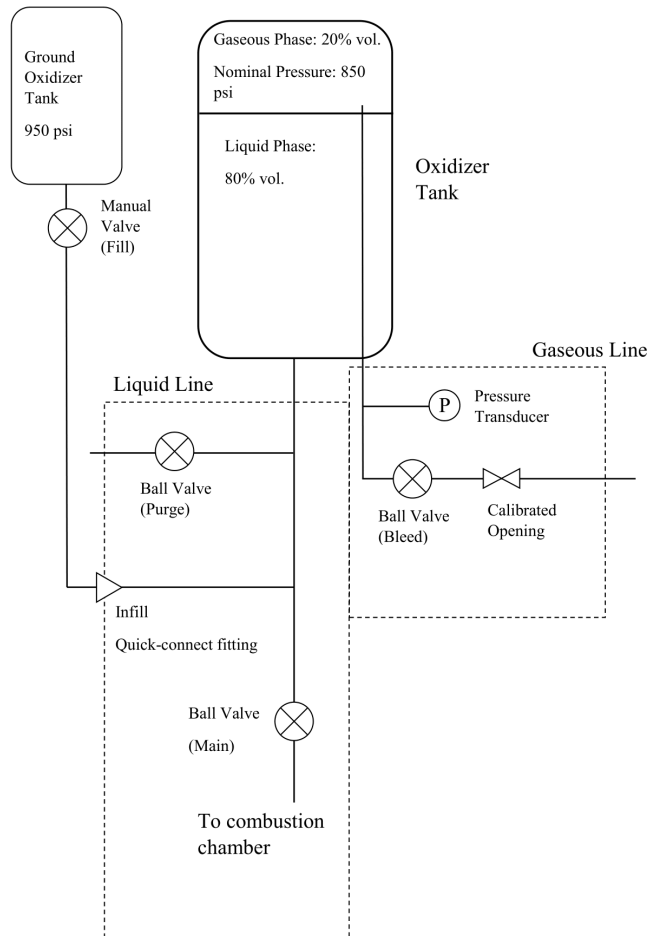


Figure 16: Oxidizer Supply System

Several static fire tests were done. Two of them were done in October 2016 using a sub-scale model of the hybrid rocket motor. Three tests were done with the full-scale motor, but the first one used different additives than those used in competition. Results of the two static tests with the right additives were presented in this technical report. Results are presented in table 6.

Table 6: Results of various tests

Test	Total Impulse [Ns]	Avg. Thrust [N]	Isp [s]	Burn time [s]
Autumn 2017	4227	1300	121	3.25
Winter 2018	4275	1016	70	4.20

Since the pressure vessel is commercial, no SRAD pressure vessel tests were done. The combustion chamber used for this motor is a Cesaroni 98mm Casing. Static fire tests were done using this combustion chamber.

VII. Appendix 3: Hazard Analysis

The pyrotechnics used for parachute ejection are very commonly used and are standard in the rocketry community. As the motor is hybrid, the fuel and oxidizer are separate until the motor firing, greatly reducing the risk of accidental ignition. The risks that they pose are included in Appendix 4 : Risk Assessment. Furthermore, special care has been taken to address those risks in the checklists presented in Appendix 5. This is to ensure the operation of the rocket is safe. Also, the team refers to a faculty advisor, Pierre Laurendeau, who has significant experience with rockets and rocket motors, as he has L3 certification and has been flying rockets as a hobby for over 20 years, including hybrid rockets. He also served as Chief Range Safety Officer and President for the Canadian Association of Rocketry. His help is very much appreciated in all aspects of the project.

VIII. Appendix 4: Risk Assessment

THIS PAGE INTENTIONALLY LEFT BLANK

Risk	Possible Causes	Risk of Mishap and Rationale	Mitigation Approach	Risk of Injury after Mitigation
PHASE 1 - ROCKET ON LAUNCH RAMP				
Explosive separation during assembly or prelaunch, causing injury	<ul style="list-style-type: none"> Deployment based on instrumentation readings and indications. Inadvertent ignition of black powder charges (possibly due to static electricity) 	Low	<ul style="list-style-type: none"> Rocket is provided live current only when on the launch rail Safety equipment will be worn by all members approaching the rocket All recovery charges shunted until rocket is on pad 	Very Low
Pyrotechnically initiated tender descenders accidentally released on ground	<ul style="list-style-type: none"> Deploy signal wrongly sent from onboard computers Spark ignites black powder charge 	Low	<ul style="list-style-type: none"> Black powder is ignited by a 5Ω resistor instead of an electronic match, requiring a very high current to generate enough heat Onboard electronics are only activated on the ramp Safety equipment will be worn by all members approaching the rocket 	Very Low
Explosion of lithium polymer batteries, causing injury	<ul style="list-style-type: none"> Battery failure Overcharging 	Low	<ul style="list-style-type: none"> Use of overcurrent, overvoltage, undervoltage and overcharge protection Avionics team has considerable experience with lithium polymer batteries High quality lithium polymer batteries will be used 	Very Low
Rocket falls from launch rail during prelaunch preparations, causing injury.	<ul style="list-style-type: none"> Poorly attached rail buttons Unpredicted roll during launch 	Medium	<ul style="list-style-type: none"> Security factor of at least 3 for rail buttons Passively controlled flight, no roll during launch 	Low
PHASE 2 - POWERED FLIGHT				

Combustion chamber explodes during flight, damaging rocket and/or altering trajectory towards personnel	<ul style="list-style-type: none"> Fuel grain ruptures, blocking nozzle Combustion chamber material failure 	Medium	<ul style="list-style-type: none"> Multiple prior tests prove motor's reliability Grain fabrication method perfected to ensure structural integrity Visually inspected motor grain for cracks, debonds, and gaps before, during and after assembly Use ductile (non-fragmenting) material for motor case Inspected motor case for damage during final assembly before launch Launch crew outside safety perimeter Combustion chamber is commercially manufactured and rated to safe pressure 	Very
Oxidizer tank or tubing rupture, damaging rocket and projecting debris.	<ul style="list-style-type: none"> Oxidizer overpressure due to heat 	Low	<ul style="list-style-type: none"> Live pressure transducer monitoring Bleed valve permits pressure relief In case of uncontrolled pressure buildup, purge valve IS opened to completely empty rocket Launch scheduled in morning to minimize solar heat Personnel within security perimeter while tank is filled wear appropriate safety equipment Tank and tubing are rated for at least 1000 psi higher than nominal pressure; tank at 2500 psi and tubing at 2000 psi. 	Very Low
PHASE 3 AND 4 - BALLISTIC FLIGHT & COASTING FLIGHT				
Rocket deviates from nominal flight path, comes in contact with personnel at high speed	<ul style="list-style-type: none"> Unstable rocket during flight Weathercocking too important (High winds, ramp clearing velocity too low, etc.) 	Medium	<ul style="list-style-type: none"> Stable rocket with 2 calibers of static margin Fins installation using a high precision, laser cut template Dynamic analysis to better understand and predict rocket behavior in all flight regimes Canceling launch if wind speed exceeds 20 mph Launch rail clearing speed at least 70 mph 	Very Low
Rocket loses one or more fins, causing an unpredictable trajectory that can potentially result in a contact with personnel at high speed	<ul style="list-style-type: none"> Fin flutter Loss of fin structural integrity 	Low	<ul style="list-style-type: none"> Extensive structural dynamic analysis of the fins Fins are full 8HS carbon fiber, radically increasing stiffness 	Very Low

Rocket disintegrates during flight and high speed debris comes in contact with personnel	<ul style="list-style-type: none"> Structural integrity insufficient 	Low	<ul style="list-style-type: none"> Extensive structural dynamic analysis Validation of fabrication processes and material through destructive tests Security margin of at least 4 	Very Low
PHASE 5, 6 & 7 - APOGEE, DROGUE CHUTE DESCENT AND MAIN CHUTE DESCENT				
Shock cord rupture during separation	<ul style="list-style-type: none"> Poorly attached shock cord Shock cord not strong enough Eyebolt or other linking devices not strong enough or poorly attached 	Low	<ul style="list-style-type: none"> Shock cord attached with heavy duty links Links tested for predicted loads including safety factors Shock cord with present end loops Shock cord chosen with a security margin of 4 Use of swivels at sections junctions with shock cord Use of Z-Fold packaging method on shock cord 	Very Low
Recovery system fails to deploy, rocket or payload comes in contact with personnel	<ul style="list-style-type: none"> Inaccurate altimeter readings Sections that are designed to separate are fitted too tight Avionics failure Both charges are not detonated 	Medium	<ul style="list-style-type: none"> Use of several altimeters to increase accuracy and redundancy Extensive testing for separation and avionics Use of shear pins for a more predictable behavior 	Very Low
Recovery system partially deploys, rocket or payload comes in contact with personnel	<ul style="list-style-type: none"> Separation section attached too tight Avionics failure Mistake during chutes folding procedure Recovery system fails to release main parachute 	Medium	<ul style="list-style-type: none"> Extensive testing for separation and avionics Extensive testing and improvement of parachute folding techniques Fully redundant parachute deployment system, with commercial and custom detonators 	Very Low

Main parachute deploys at or near apogee, rocket or payload drifts far away	<ul style="list-style-type: none"> Tender descender fails to tether the main parachute to the rocket Main parachute comes loose during flight 	Medium	<ul style="list-style-type: none"> Tender descender system tested and validated to the maximum predicted shock load and twice the maximum operating load Use of a deployment bag for the main parachute 	Low
PHASE 8 - LANDING				
One or more explosive charges exploded once the rocket is on the ground, causing injury to the recovery team	<ul style="list-style-type: none"> Avionics failure Igniter failure 	Low	<ul style="list-style-type: none"> Black powder is ignited by a 5Ω resistor instead of an electronic match, requiring a very high current to generate enough heat Live current in the rocket can be turned off by turning an easily accessible switch Safety equipment will be worn by all members approaching the rocket The avionics bay is automatically set to "safe mode" when the rocket has landed, which prevents any detonation of unburnt charges 	Very Low

IX. Appendix 5: Assembly, Preflight and Launch Checklists

THIS PAGE INTENTIONALLY LEFT BLANK

Preflight checklist

Prometheus

Oronos Polytechnique Montréal

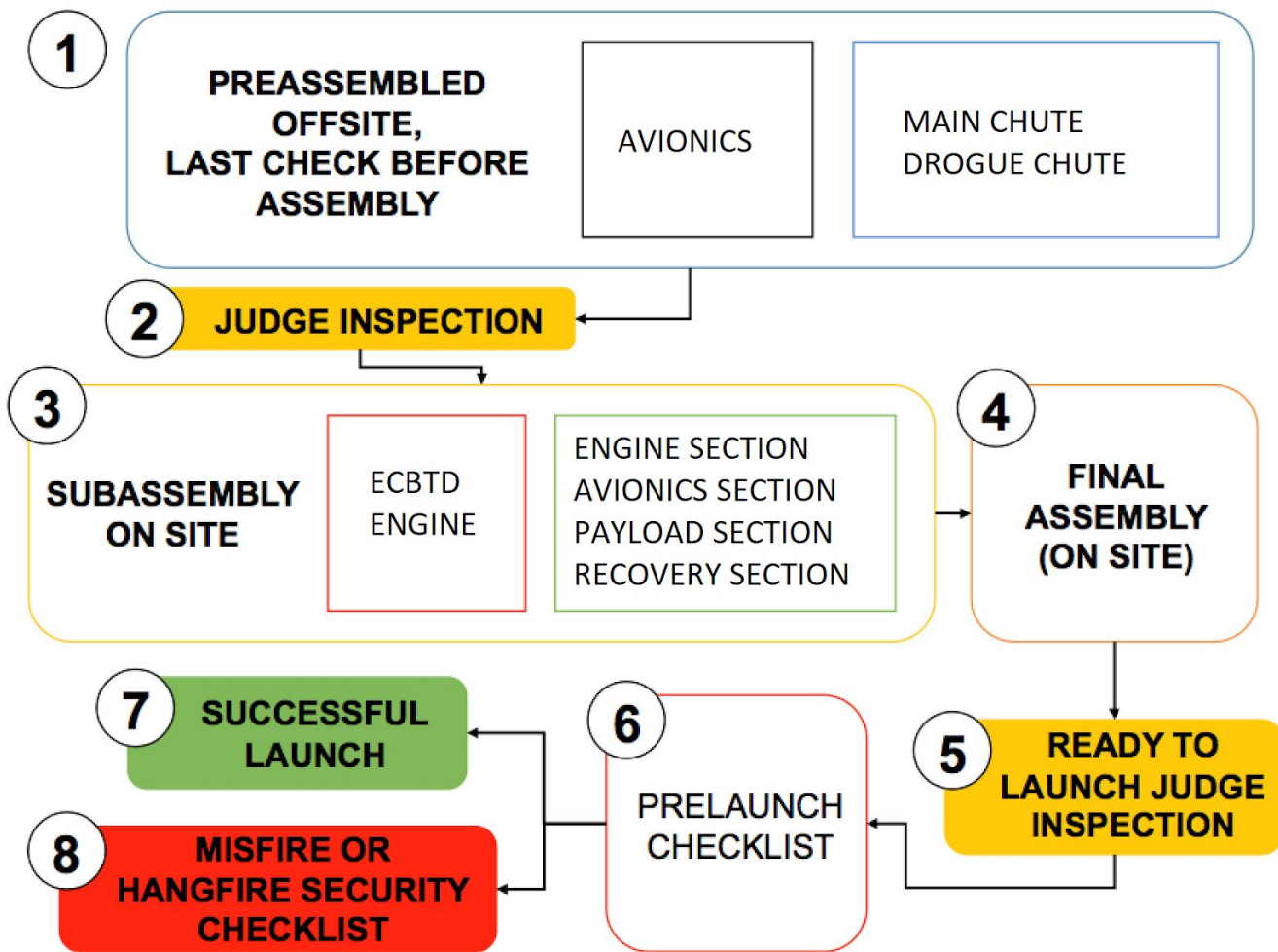
Team 59

IREC 2018

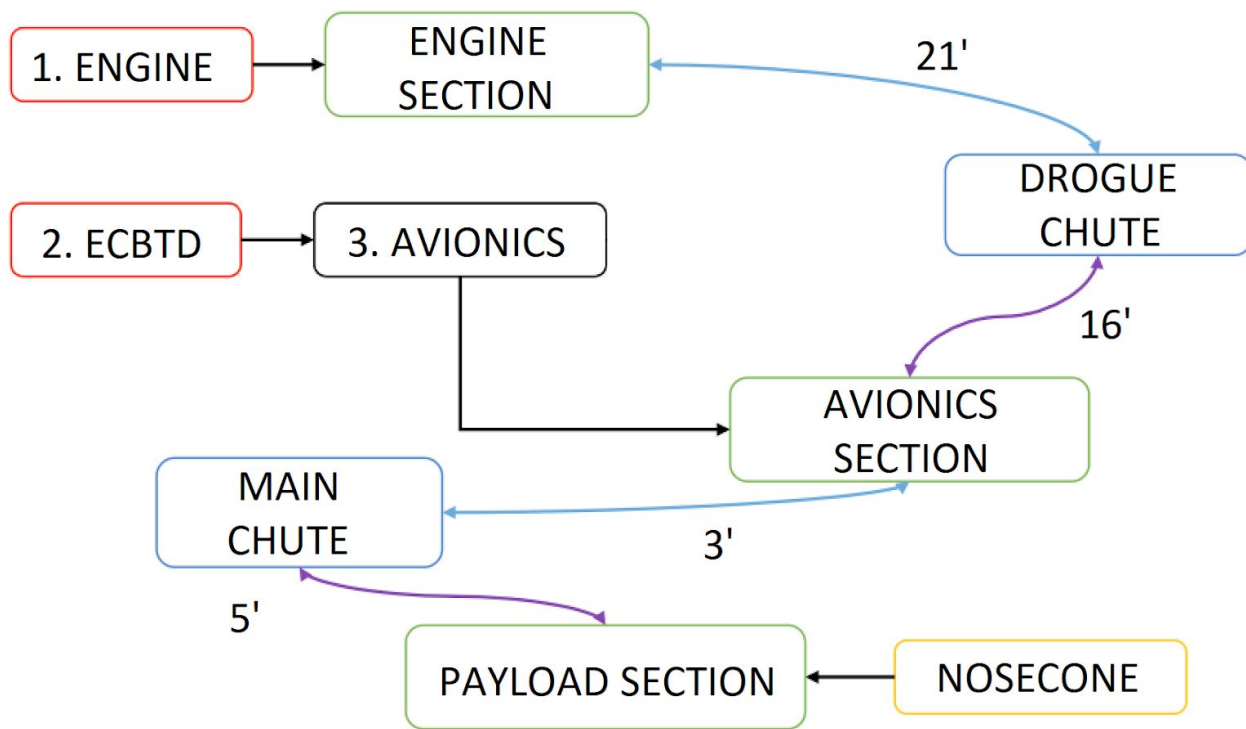
Spaceport America, New Mexico, USA

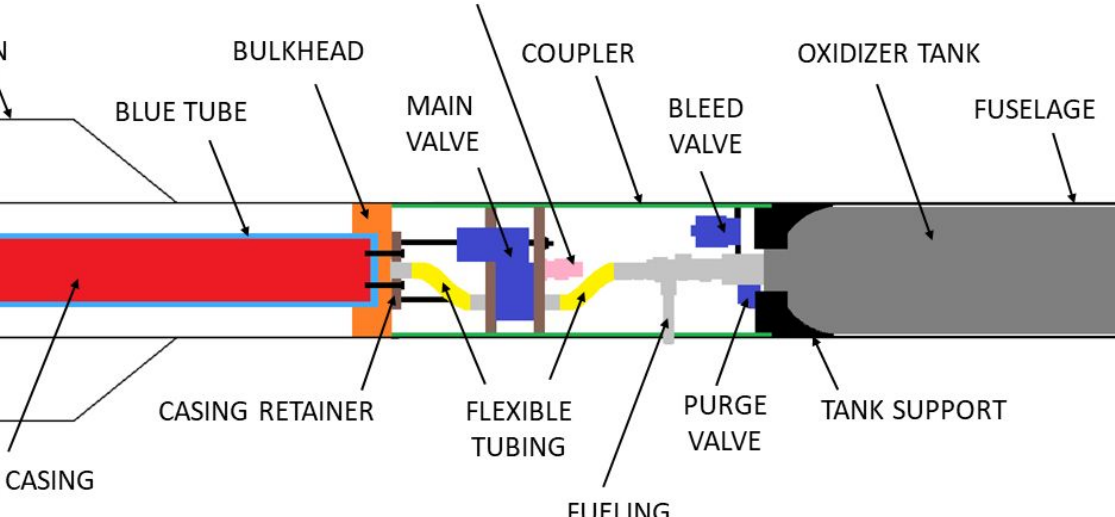
Task	Team Member
Team Leader	Olivier JOBIN
Overseer	Pierre LAURENDEAU
Checklist Supervisor	Mathieu CHARTRAY-PRONOVOST
Avionics Software Specialist	Youva CHEMAM
Avionics Hardware Specialist	Nathanaël BEAUDOIN-DION
Engine Assembly Specialist	Pablo PONCE-JULIEN
Engine Assembly Support	Guillaume VILLENEUVE
Ground Support Specialist	Youva CHEMAM
Recovery Specialist	Charles BILODEAU-BÉRUBÉ
Recovery Support	Pablo PONCE-JULIEN
Engine Specialist & Safety Officer	Olivier JOBIN
Engine Support	Mathieu CHARTRAY-PRONOVOST

Workflow chart



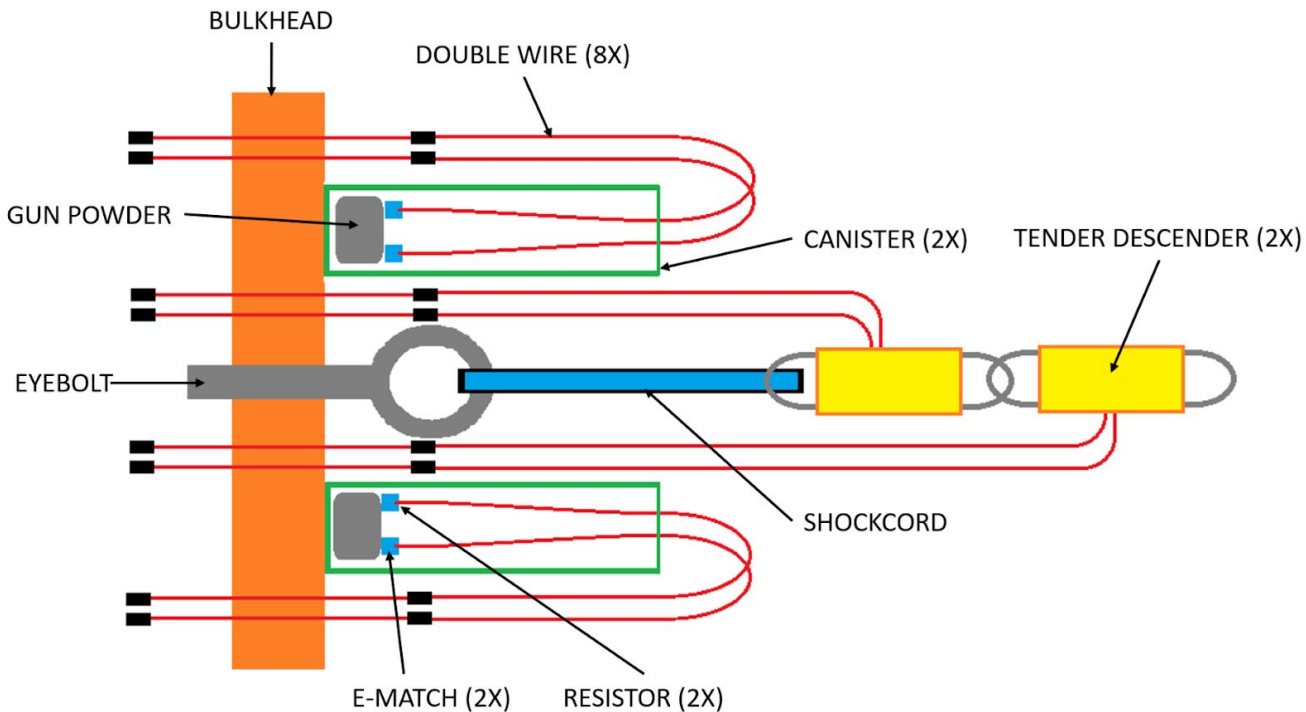
Assembly layout



SUBASSEMBLY ONSITE	X
1. Engine Section	
 <p>The diagram illustrates the internal components of the engine section. It shows a red motor casing at the bottom, connected to a blue tube and a phenolic tube. The phenolic tube passes through a bulkhead and is secured by a casing retainer. At the top, there is an avionics connector, a main valve, and a coupler. A flexible tubing connects the engine head to the fueling quick-connect. Bleed and purge valves are located near the tank support. The oxidizer tank is shown on the right, connected to the engine section. The diagram also indicates the AFT and FORE directions.</p>	
<ol style="list-style-type: none"> 1.1. Glue the fuel grains inside the phenolic tube 24 hours before assembly 1.2. Glue the ignition engine WITHOUT the electric match 24 hours before assembly 1.3. Lubricate four o-rings (two for the engine head, one for the engine head cap and one for the swirl injector (orange o-ring)) and the four-hole gasket using Krytox or Vaseline 1.4. Lubricate the outside of the engine head cap 1.5. Place the o-rings on the engine head and the engine head cap 1.6. Place the orange o-ring on the swirl injector 1.7. Place the swirl injector at the bottom of the narrow section of the engine head (larger side of the swirl injector pointing up) 1.8. Lubricate and place an o-ring on the narrow section of the engine head 1.9. Place the retaining ring (dark) on the narrow section of the engine head 1.10. Screw the engine head into the motor casing on the opposite end of the white tape. Screw until the retaining ring (dark) and the casing lie on the same plane (flush) 1.11. PUSH the engine head cap to the bottom of the narrow section of the engine head 1.12. Connect the bottom flexible tubing to the engine head 1.13. Insert the phenolic tube in the motor casing 1.14. Insert the nozzle at the bottom of the motor casing 	

1.15.	Insert an o-ring on the nozzle and screw the AFT. nozzle retainer on the engine casing	
1.16.	Insert the engine casing with the bottom flexible tubing in the Blue Tube	
1.17.	Place the four-hole gasket on the engine head	
1.18.	Place the four-hole metal plate on the four-hole gasket	
1.19.	Place the casing retainer on the four-hole metal plate	
1.20.	Tighten the four screws ($\frac{3}{8}$ "-16) in the injector using an Allen wrench	
1.21.	Connect and tighten the upper end of the bottom flexible tubing to the main valve	
1.22.	Connect and tighten previously assembled upper plumbing (purge valve, bleed valve, oxidizer tank) to upper end of the top flexible tubing, already connected to the main valve	
1.23.	Connect and tighten Avionics Harness to Avionics Connector on top of the main valve	
1.24.	Slide the coupler along the oxidizer tank and plumbing until resting against the bulkhead	
1.25.	Install the two-piece tank support underneath the oxidizer tank and secure position onto the coupler	
1.26.	Screw the two pieces of the tank support together using $\frac{1}{4}$ "-20 screws and bolts, and washers	
1.27.	Slide the fuselage over the oxidizer tank and coupler	
1.28.	Tighten the four 8-32 screws through the fuselage and coupler against the bulkhead to secure them together	
1.29.	Connect and tighten the fueling quick-connect to the plumbing assembly	
1.30.	Connect and tighten the calibrated opening to the bleed valve	
1.31.	ENGINE SECTION ASSEMBLY IS COMPLETED	
INITIALS:		

2. Ejection Canisters Bulkhead and Tender Descender (ECBTD)

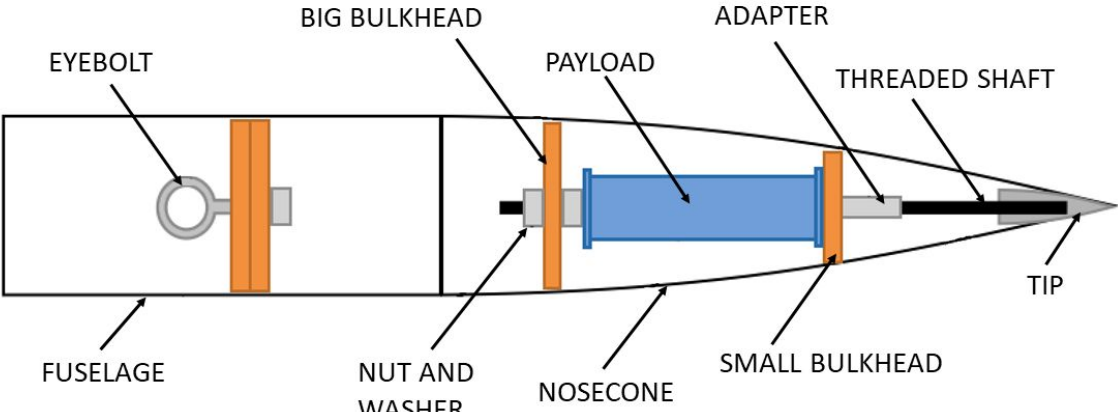


- 2.1. Verify that the eyebolt is fastened securely and attached to the shock cord
- 2.2. Put black powder in both tender descenders
- 2.3. Connect the proper wire to both tender descenders
- 2.4. Make sure all the wires for the canisters are not damaged and are connected to the e-match or resistor
- 2.5. Test all resistors using a multimeter: 5 Ohm
- 2.6. Put 1.5g of gunpowder in each canister
- 2.7. Put the resistors and e-matches inside the canister
- 2.8. Verify the wire will not block the coupler
- 2.9. Put fire retardant paper in each canister and squeeze it enough to seal the gunpowder
- 2.10. ECBTD ASSEMBLY IS COMPLETED

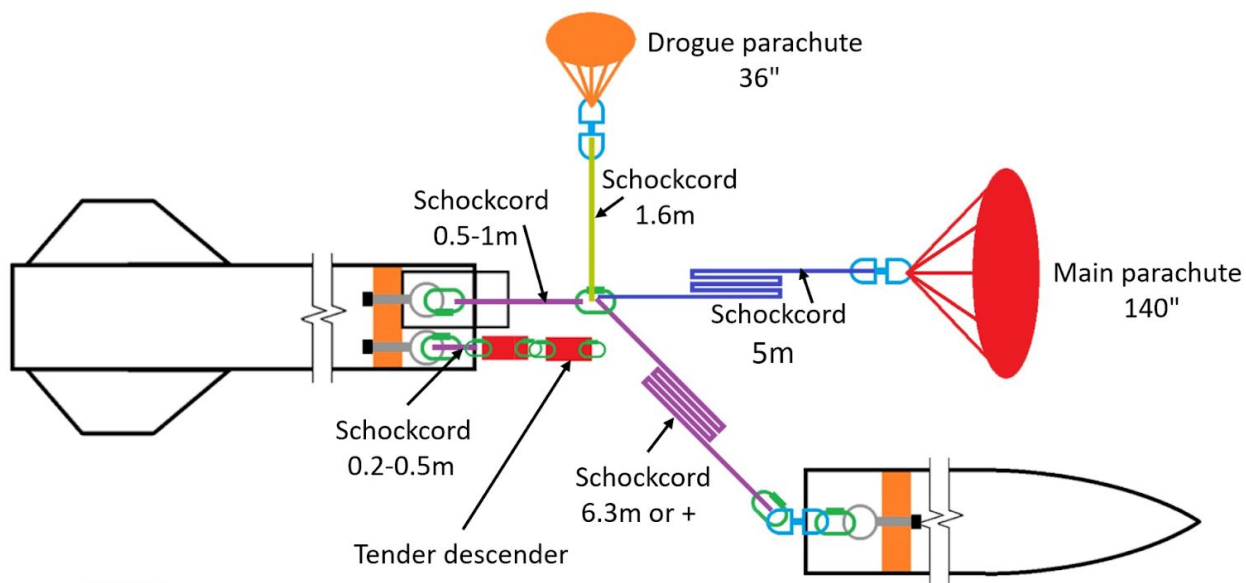
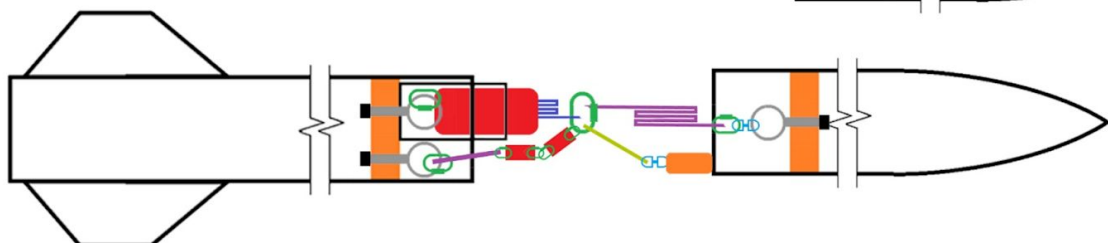
INITIALS:

3. Avionics section	
3.1. Remove any kapton from the barometers and buzzers	
3.2. Make sure SD cards are empty and formatted correctly	
3.3. Insert SD cards in the PCBs (3 in total)	
3.4. Connect all recovery harnesses including resistor detonators, NO BLACK POWDER IN CANISTERS	
3.5. Insert the avionics bay in rocket	
3.6. Screw the avionics case from outside of the rocket, 4 screws	
3.7. Install dummy 5 Ohm resistors instead of both StratoLoggers' e-matches	
3.8. Put the knob on the switch	
3.9. Put the switch on position #1	
3.10. All electronics systems are SHUT DOWN. NO LIGHT, NO SOUND	
3.11. Put the switch on position #2	
3.12. Listen to the diagnostic of the StratoLogger #1	
3.12.1. Verify: at all times, no siren tone	
3.12.2. Verify: beeping sequence is:	
3.12.2.1. Short beep 1x - long pause	
3.12.2.2. Short beep 1x - pause - 5x - pause - 1x - pause - 1x - long pause	
3.12.2.3. Long beep (only if StratoLogger number is 2) - long pause	
3.12.2.4. Short beep<last altitude> - long pause	
3.12.2.5. Short beep<battery voltage> - long pause	
3.12.2.6. Triple beeps with short pause between in a loop.	
3.12.3. Verify: reported battery voltage is greater than 8.8V	
3.13. Put the switch on position #3	
3.14. Listen to the diagnostic of the StratoLogger #2 (follow the same procedures as StratoLogger #1)	
3.15. Put the switch on position #4	
3.16. Establish telemetry link with avionics	
3.16.1. Verify: all statuses GREEN	
3.16.2. Arm the avionics	
3.16.3. Verify: arming status RED , all other statuses GREEN	
3.16.4. Disarm the avionics	
3.16.5. Open the Hanbay valve and confirm its opened status	
3.16.6. Close the Hanbay valve and confirm its closed status	
3.16.7. Open and close bleed valve and auditorily confirm its status with the clicking sound	
3.16.8. Open and close purge valve and auditorily confirm its status with the clicking sound	
3.17. Put the switch on position #1	
3.18. Take off the knob	
3.19. Remove dummy 5 Ohm resistors from both StratoLogger's outputs	
3.20. All electronics systems are SHUT DOWN. NO LIGHT, NO SOUND	
3.21. CAREFULLY Connect four (4) e-matches to the StratoLogger's outputs	

3.22. CAREFULLY load drogue parachute canisters with black powder (2.0g)	
3.23. CAREFULLY load main parachute tender descenders with black powder (0.25g)	
3.24. Close avionics section	
AVIONICS SECTION ASSEMBLY IS COMPLETED.	
INITIALS:	

4. Nosecone and Payload (ballast) section	
	
4.1. Screw the adapter with the 3/8" and 1/4" threaded shaft 4.2. Screw the 1/4" threaded shaft to the nosecone tip. 4.3. Insert the smaller bulkhead in the 1/4" threaded shaft. It must rest on the adapter. 4.4. Insert the payload and tighten with a bolt and washer. 4.5. Insert the bigger bulkhead. 4.6. Tighten with another bolt and washer. 4.7. Assemble the nosecone and the fuselage together and secure the whole with 3 screws. 4.8. PAYLOAD SECTION ASSEMBLY IS COMPLETED.	
INITIALS:	

5. Parachute section

1**2**

- 5.1. Fold the main and the drogue
- 5.2. Verify 1.6m, 5m and 6.3m shockcords are tied to a **SWIVEL-CARABINER**
- 5.3. Drogue is tied to nomex sheet (not shown on the figure)
- 5.4. Attach corresponding shockcord to the parachutes and to the fuselage (like on the figure 1)
- 5.5. Put the main parachute in the fuselage (like on figure 2)
- 5.6. Attach the tender descender to the center quicklink
- 5.7. Put the drogue parachute in the superior fuselage with the rest of the shockcord
- 5.8. Close the section
- 5.9. Payload section is tied to LPS **EYEBOLT-CARABINER-SWIVEL-CARABINER**
- 5.10. Insert shear pins **4 X #40**
- 5.11. PARACHUTE ASSEMBLY IS COMPLETED.

INITIALS:

Preflight signatures

Validation	ESRA member name	Signature	Date
Payload			
Wiring			
Ready to launch			

Checklist is completed:

Name:

Signature:

Date:

FUELING AT LAUNCH PAD	X
6. FUELING	
6.1. Material in hand:	
6.1.1. Nitrous Oxide Tank	
6.1.2. Wrench	
6.1.3. Pen & Checklist	
6.1.4. Face shield	
6.2. Previous preflight checklist is completed	
6.3. Pull down the ramp.	
6.4. Slide the rocket on the ramp with the rail buttons.	
6.5. Raise the ramp at 85° angle minimum.	
6.6. Non-essential personnel left the launch pad - Team Leader, Overseer, Checklist Supervisor, Engine Specialist & Safety Officer and Avionics Hardware Specialist MUST STAY	
6.7. Tip over the refueling tank while keeping it stable. The exit valve of the refueling tank must face downwards. The refueling tank must remain in this position until step 6.17	
6.8. Open the bleeding valve	
6.9. Open the valve connecting the refueling and motor tanks. The motor tank is now filling up	
6.10. Confirm that the motor tank is filling by observing gas escaping from the bleeding hole.	
6.11. Maintain the refueling tank in its upside down position. When the motor tank is 75% full, liquid will escape instead of gas.	
6.12. Close the valve connecting the refueling and motor tanks	
6.13. Close the bleeding valve	
6.14. Place the refueling tank back into a stable position	
6.15. Wait for the confirmation of ESRA to proceed to the launch operations	

PRELAUNCH AT LAUNCH PAD		X
7. Prelaunch		
7.1. Material in hand:		
7.1.1. Igniter		
7.1.2. Igniter installation kit on the rocket		
7.1.3. Multi-tool		
7.1.4. Multimeter		
7.1.5. Walkie-talkie		
7.1.6. Pen & Checklist		
7.1.7. Face shield		
7.1.8. Laptop with telemetry antenna		
7.1.9. Two (2) knobs for switch		
7.2. Previous preflight checklist is completed		
7.3. Connect the four (4) thermistors at the bottom of the rocket.		
7.4. Put the knob on the switch		
7.5. Put the switch on position #1		
7.6. All electronics systems are SHUT DOWN. NO LIGHT, NO SOUND		
7.7. Verify electrical continuity in igniter (outside of engine).		
7.8. Igniter is inserted in engine		
7.9. Igniter is shorted		
7.10. Prior to connection, make sure e-match is shorted.		
7.11. Put the switch on position #2		
7.12. Listen to the diagnostic of the StratoLogger #1		
7.12.1. Verify: at all times, no siren tone		
7.12.2. Verify: beeping sequence is:		
7.12.2.1. Short beep 1x - long pause		
7.12.2.2. Short beep 1x - pause - 5x - pause - 1x - pause - 1x - long pause		
7.12.2.3. Long beep (only if StratoLogger number is 2) - long pause		
7.12.2.4. Short beep<last altitude> - long pause		
7.12.2.5. Short beep<battery voltage> - long pause		
7.12.2.6. Triple beeps with short pause between in a loop.		
7.12.3. Verify: reported battery voltage is greater than 8.8V		
7.13. Put the switch on position #3		
7.14. Listen to the diagnostic of the StratoLogger #2 (follow the same procedures as StratoLogger #1)		
7.15. Put the switch on position #4		
7.16. Remove the knob		
7.17. Establish telemetry link with avionics		
7.17.1. Verify: all statuses GREEN		
7.17.2. Confirm with telemetry: all four (4) thermistors are detected		
7.17.3. Arm the avionics		
7.17.4. Verify: arming status RED , all other statuses GREEN		

7.18. Connect igniter to power wires	
7.19. Everyone has left the launch pad	

LAUNCH SEQUENCE	
8. Prelaunch	
8.1. Material in hand:	
8.1.1. Walkie-talkie	
8.1.2. Laptop with telemetry antenna	
8.2. Establish telemetry link with avionics	
8.2.1. Verify: arming status RED , all other statuses GREEN	
8.2.2. Verify: all thermistors are detected	
8.2.3. Enable launch auto-sequence mode	
8.2.4. Verify: launch auto-sequence mode is enabled	
IF YES, PROCEED TO NEXT STEPS	
IF NO, DO NOT LAUNCH	
8.3. Notify range officials the rocket is GO FOR LAUNCH	
8.4. Let range officials press the launch button	
8.5. Enjoy	

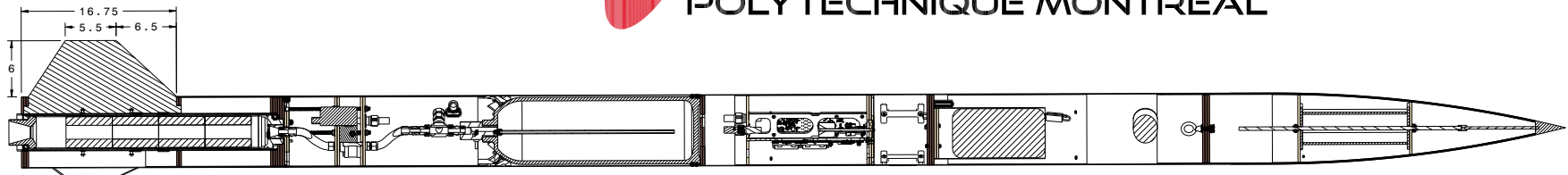
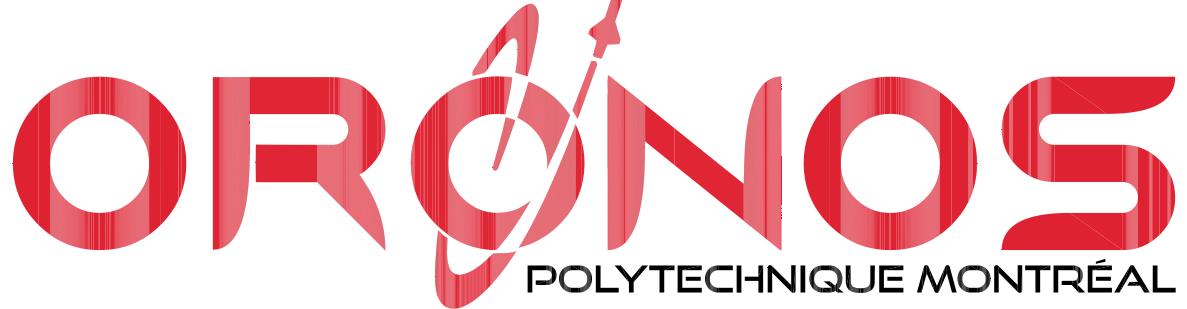
LAUNCH TROUBLESHOOTING		X
9.	Nothing happens	
9.1.	Material in hand:	
9.1.1.	Spare igniter	
9.1.2.	Igniter installation kit on the rocket	
9.1.3.	Multitool	
9.1.4.	Multimeter	
9.1.5.	Walkie-talkie	
9.1.6.	Face shield	
9.2.	Wait 5 minutes	
9.3.	Disarm avionics via software. NO BEEPS CAN BE HEARD	
9.4.	Turn off StratoLoggers (arming key to max counterclockwise). NO BEEPS CAN BE HEARD	
9.5.	Approach the rocket - NITROUS OXIDE IS IN THE TANK, FACE SHIELD MUST BE WORN	
9.6.	Disconnect igniter from power wires	
9.7.	Remove igniter (May need 2 extra persons to lift the rocket, depending on ramp height)	
9.8.	Verify if igniter has burned	
IF YES, GO BACK TO STEP 7.4 (PREVIOUS PAGE)		
IF NO, FOLLOW NEXT INSTRUCTIONS		
9.9.	Advise range safety officer that non-ignition may be caused by electrical ignition system malfunction	
9.10.	Nitrous Oxide is purged	
9.11.	Red cap is removed	
9.12.	Remove igniter	
9.13.	Go back to 6.6	

RECOVERY SAFETY PROCEDURE		X
10.	Main parachute not deployed or both parachutes deployed	
10.1.	StratoLoggers are turned off by turning the key counter clockwise NO BEEPING SOUND	
10.2.	Avionics is disarmed remotely NO BEEPING SOUND	
10.3.	If avionics cannot be disarmed, wait 12 hours for the batteries to discharge	

X. Appendix 6: Engineering Drawings

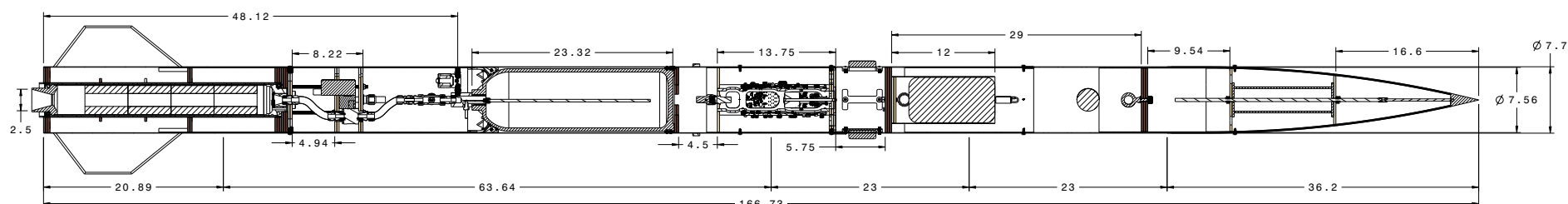
DRAWINGS START ON NEXT PAGE

The engineering drawings are provided for reference only and were scaled from their original dimensions to fit the page format used in this report. Access to the original files can be granted by contacting the author.



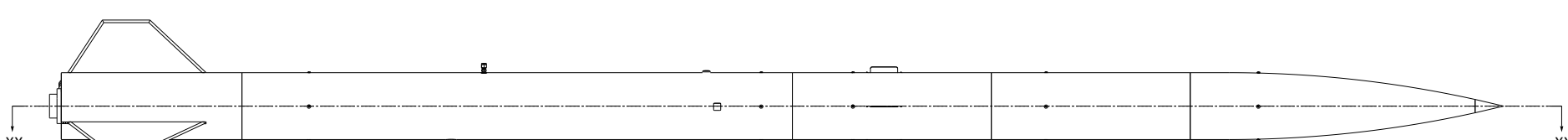
SECTION VIEW YY-YY

SCALE: 1:6



SECTION VIEW XX-XX

SCALE: 1:6



FRONT VIEW

SCALE: 1:6

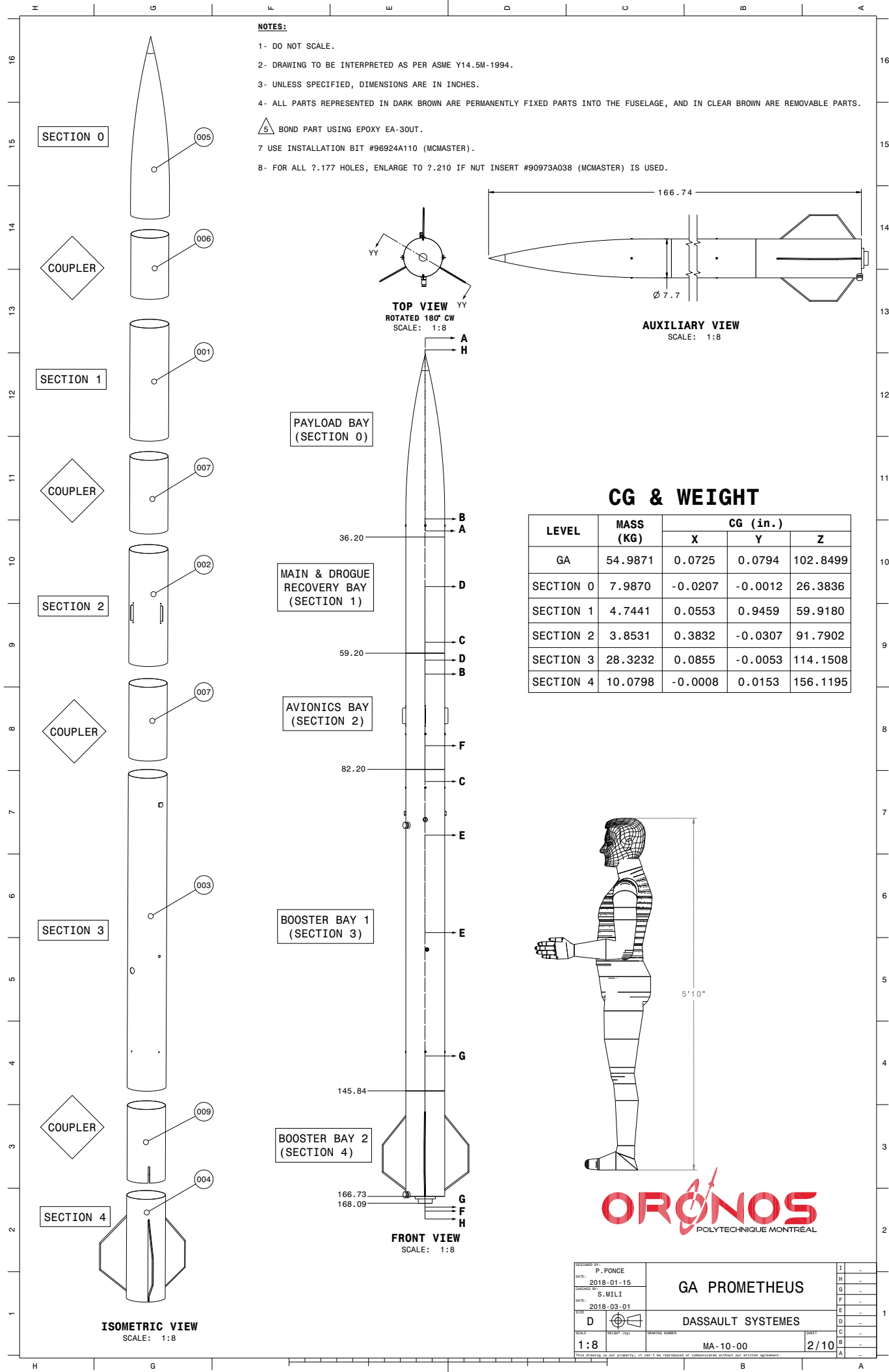


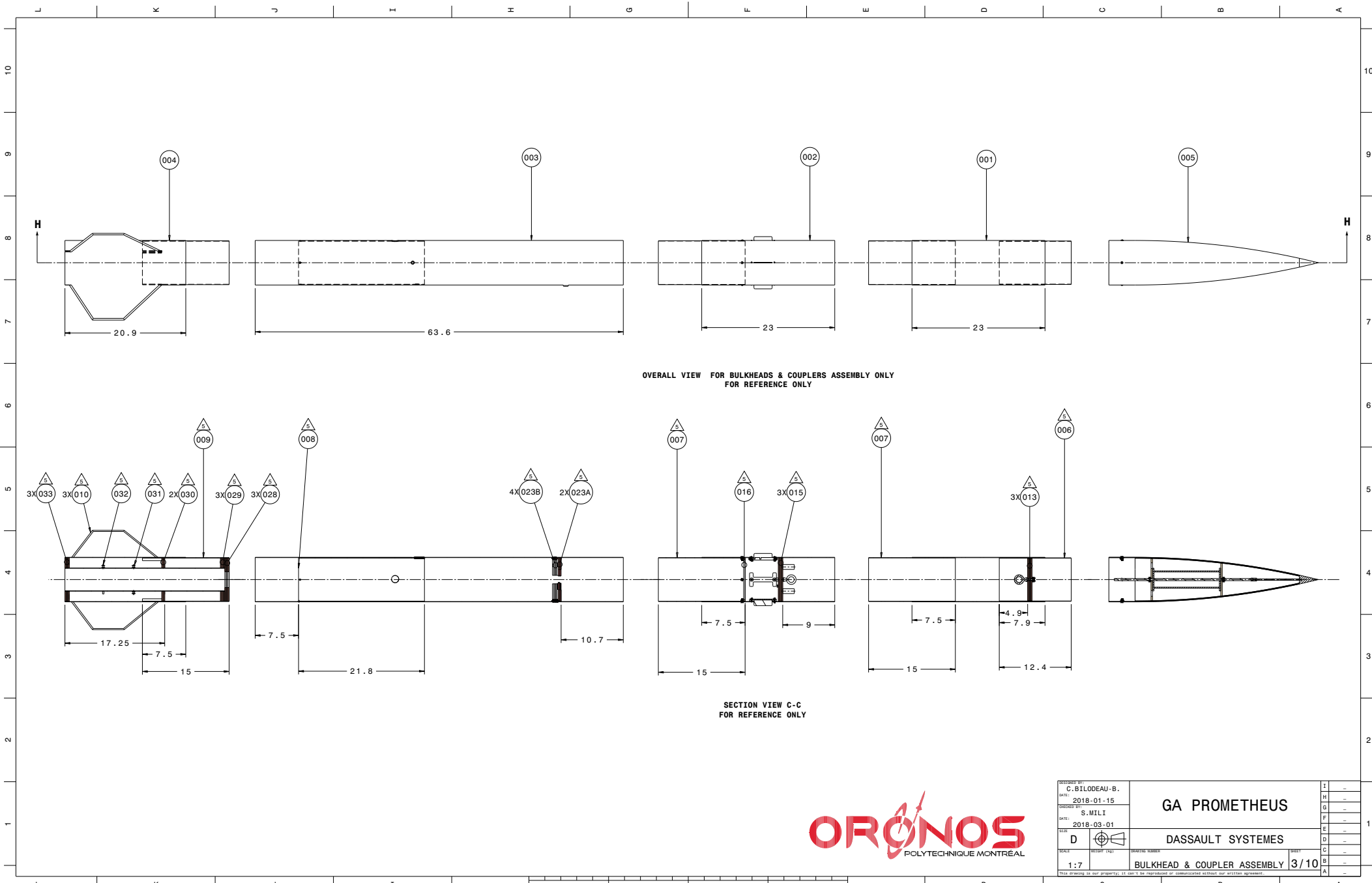
P. PONCE
DATE: 2018-01-15
CHECKED BY: S. MILI
DATE: 2018-03-01
DRAWN BY: DASSAULT SYSTEMES
SCALE: 1:6
RELEASER (142) DRAWING NUMBER: MA-10-00
DRAFTSMAKER (142) DATE: 1/10

I -
H -
G -
F -
E -
D -
C -
B -
A -

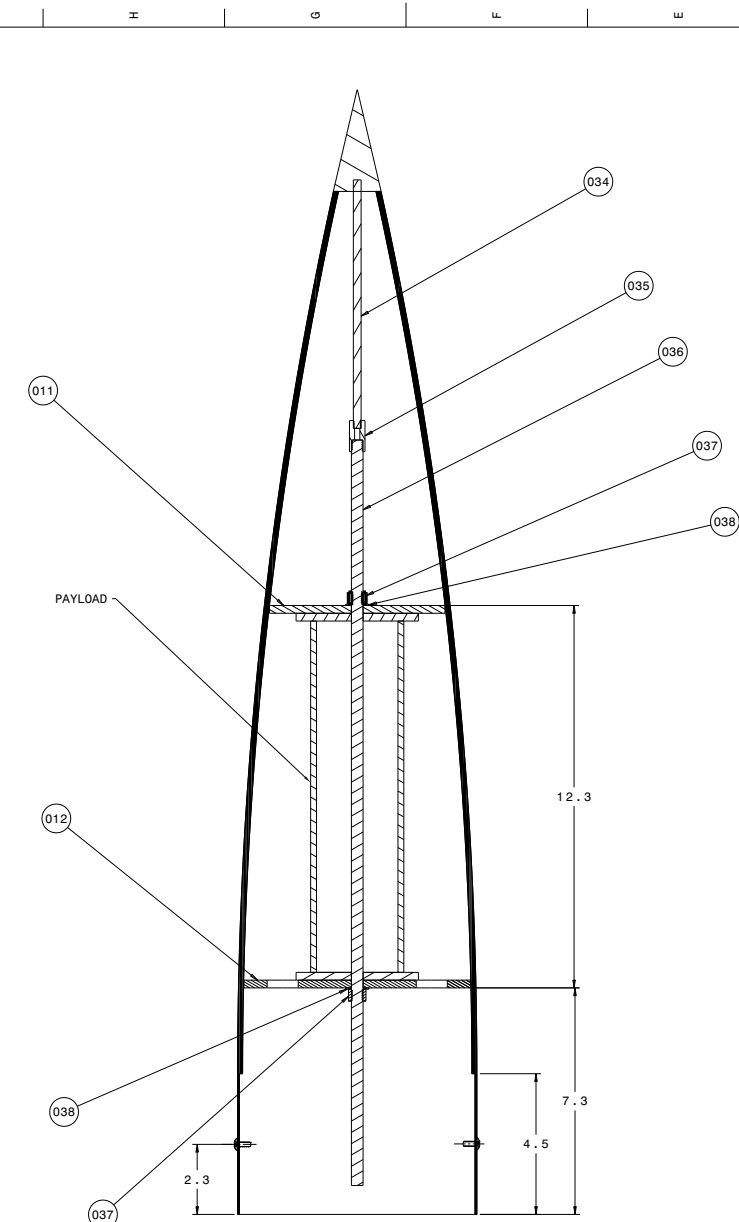
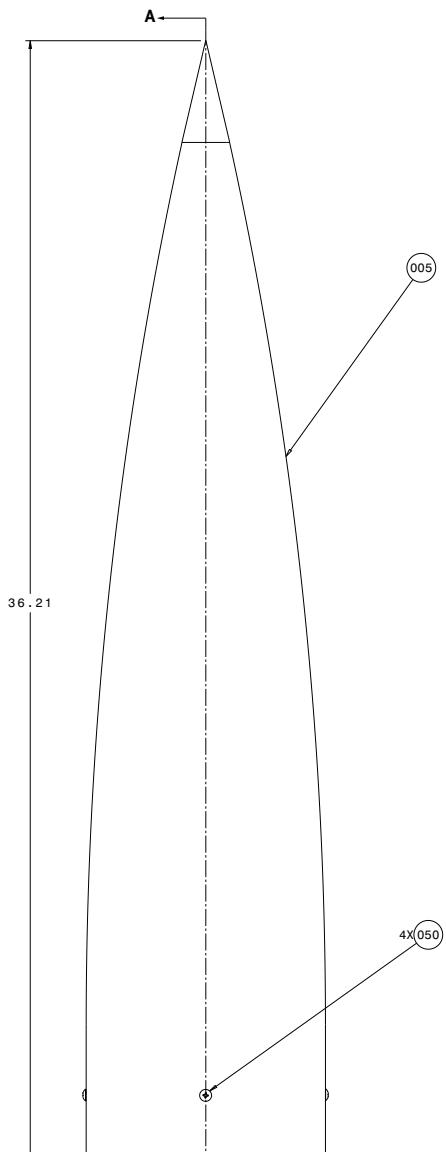
I -
H -
G -
F -
E -
D -
C -
B -
A -

This drawing is our property; it can't be reproduced or communicated without our written agreement.



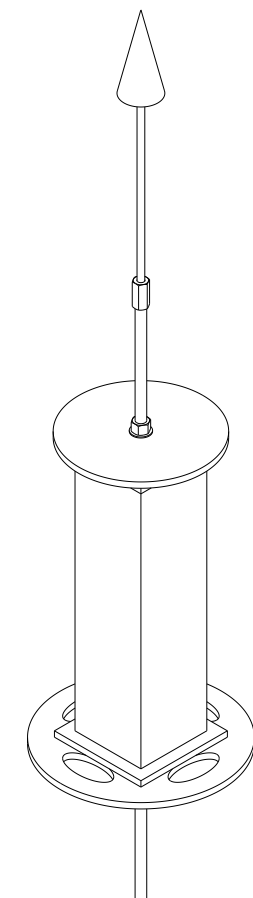


FRONT VIEW OF SECTION O
SCALE: 1:2



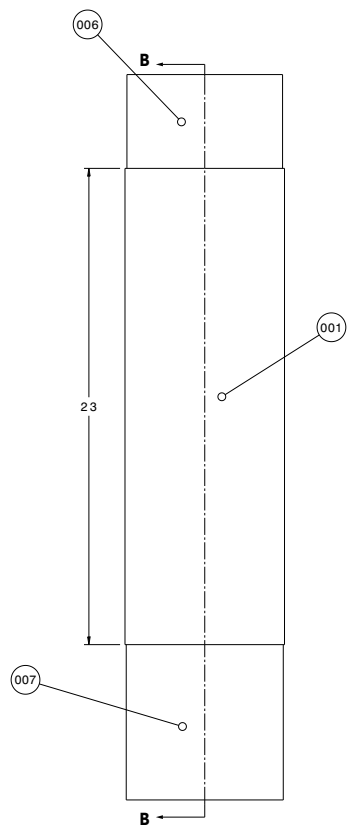
SECTION VIEW A-A
SCALE: 1:2

ORIONOS
POLYTECHIQUE MONTREAL

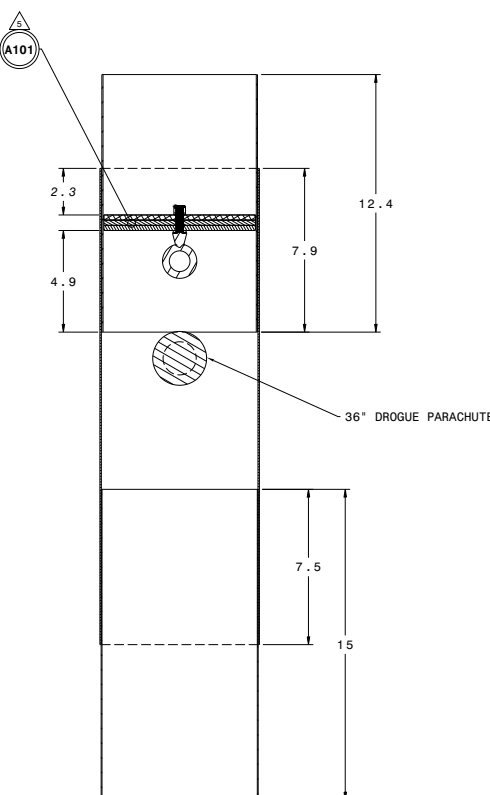


ISOMETRIC VIEW WITHOUT NOSECONNE
FOR REFERENCE ONLY

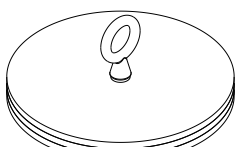
DESIGNED BY:	C.BILODEAU-B.	I	-
DATE:	2018-01-15	H	-
CHECKED BY:	S.MILLI	G	-
DATE:	2018-03-01	F	-
SCALE:	1:2	E	-
WEIGHT (kg)	142	D	-
		C	-
		B	-
		A	-
GA PROMETHEUS		I	1
DASSAULT SYSTEMES		H	-
SECTION O : PAYLOAD BAY		G	-
4 / 10		F	-
This drawing is our property; it can't be reproduced or communicated without our written agreement.			



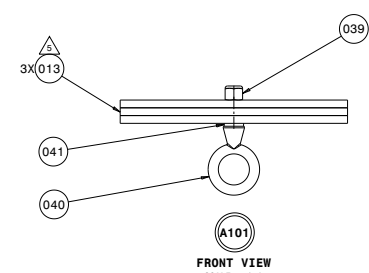
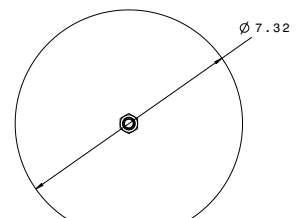
FRONT VIEW OF SECTION 1
SCALE : 1:3



SECTION VIEW B-B
SCALE: 1:3

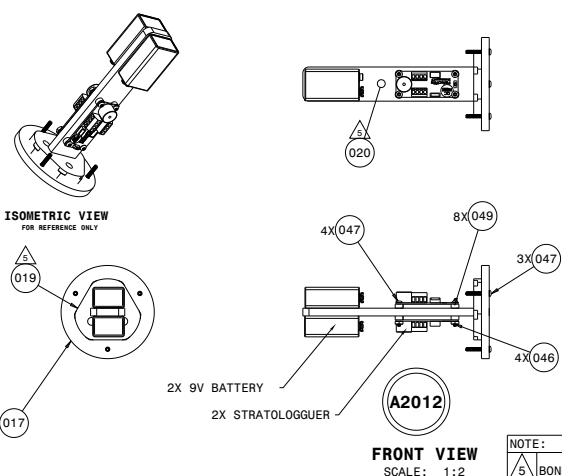
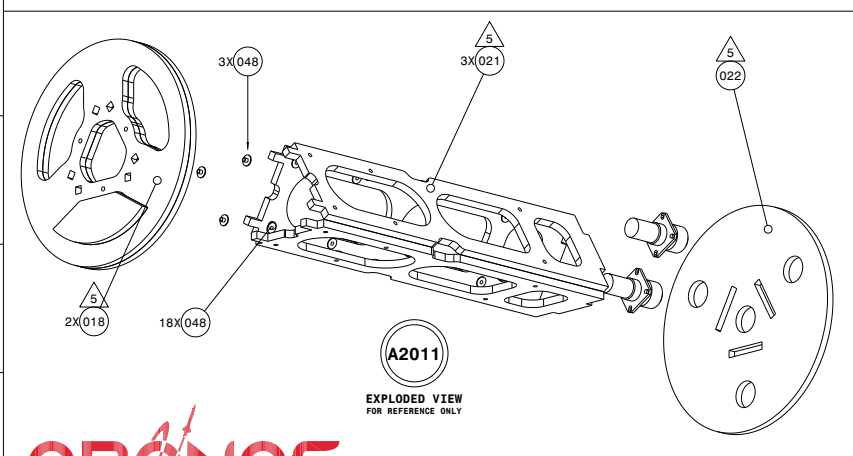
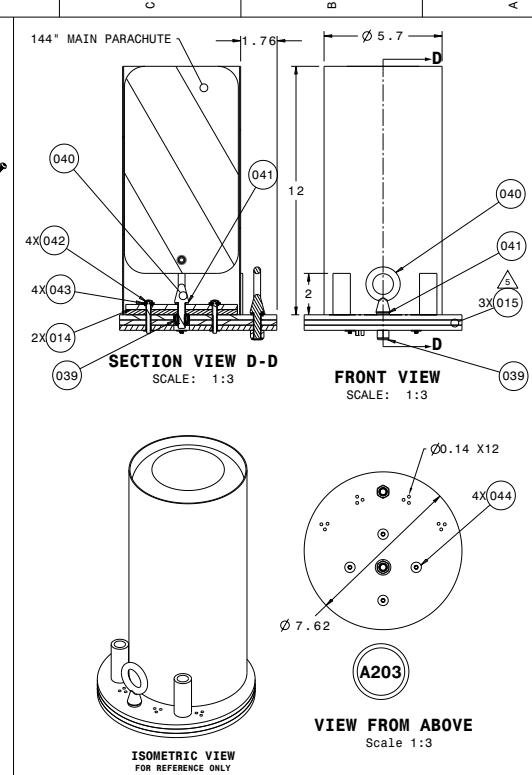
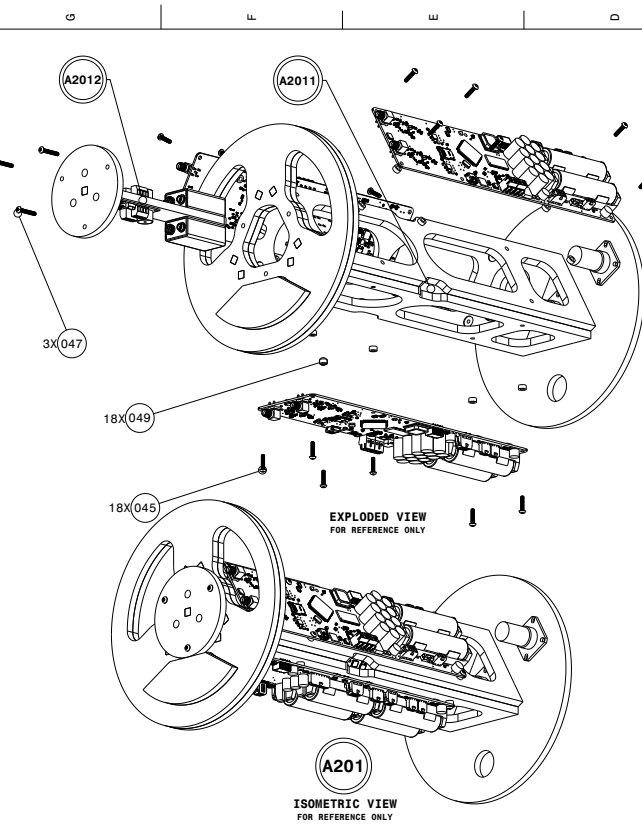
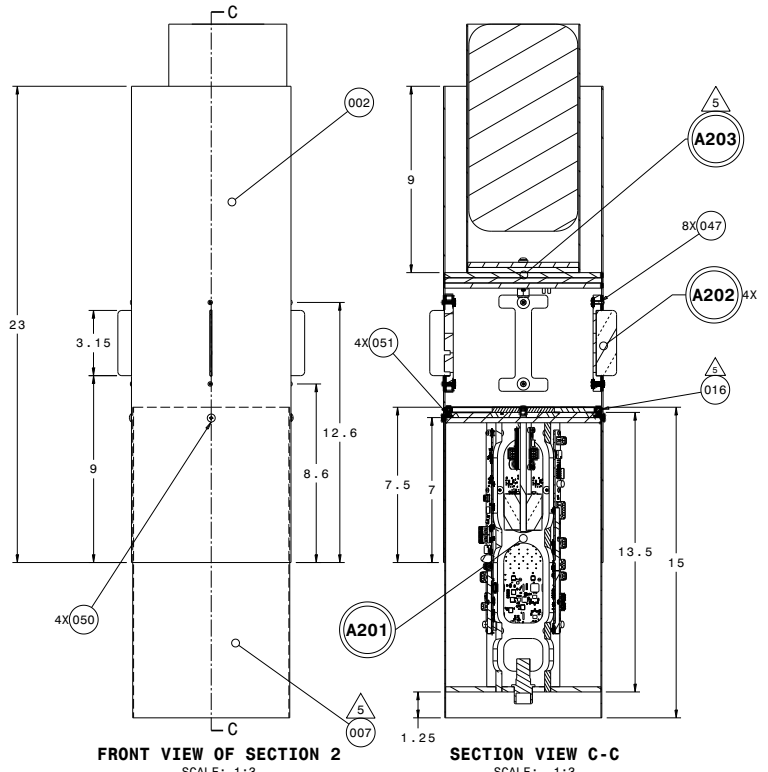


ISOMETRIC VIEW
FOR REFERENCE ONLY



ORONOS
POLYTECHIQUE MONTREAL

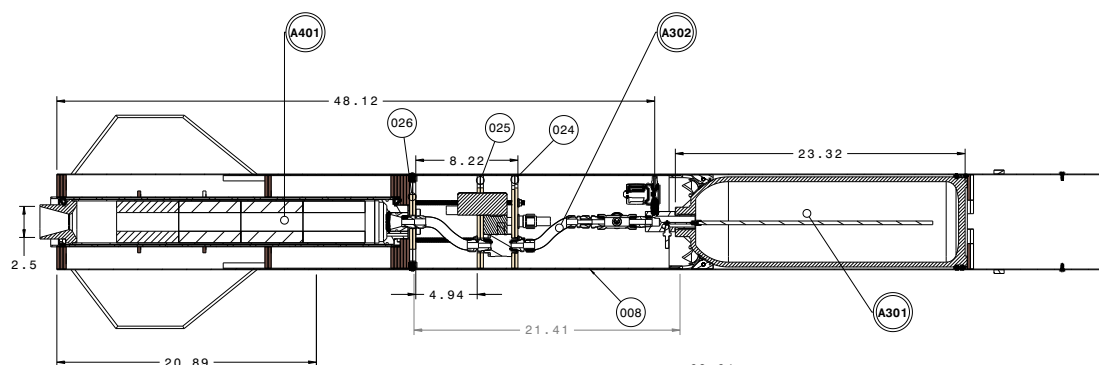
DESIGNER: C.BILODEAU-B	I -
DATE: 2018-01-15	H -
CHECKED BY: S.MILLI	G -
DATE: 2018-03-01	F -
DRAWN BY: D	E -
SCALE: 1:3	D -
	C -
	B -
	A -
GA PROMETHEUS	
DASSAULT SYSTEMES	
SECTION 1 : RECOVERY BAY	
5/10	
This drawing is our property; it can't be reproduced or communicated without our written agreement.	



DESIGNED BY:	C.BILODEAU	I	-
DATE:	2018-04-18	H	-
CHECKED BY:	S.MILI	G	-
DATE:	2018-03-01	F	-
SCALE:	D	E	-
WEIGHT (kg)	0.42	D	-
DRAWING NUMBER:		C	-
SECTION 2 : AVIONIC BAY	6 / 10	B	-
A	-	-	-

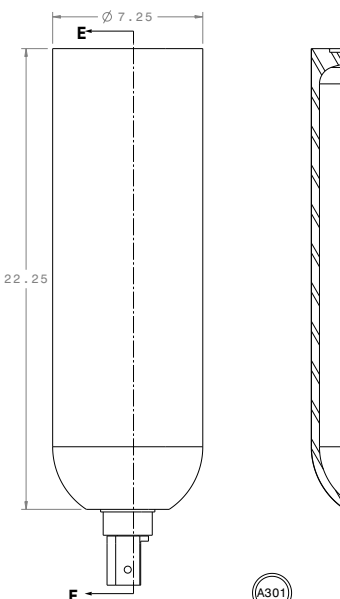
This drawing is our property; it can't be reproduced or communicated without our written agreement.

ORONOS
POLYTECHNIQUE MONTREAL

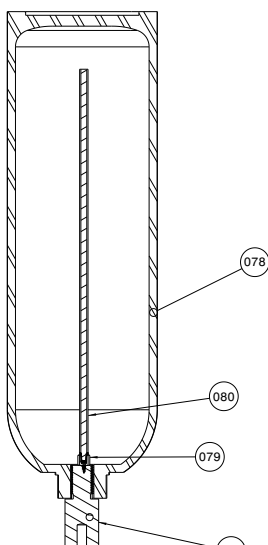


SECTION VIEW F-F

SCALE: 1:5

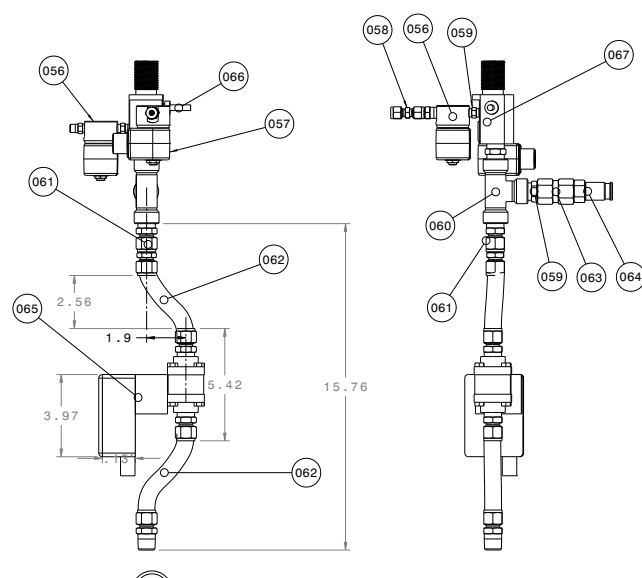


FRONT VIEW



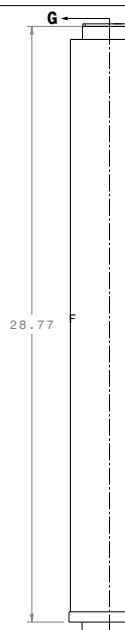
SECTION VIEW E-E

SECTION VIEW



1

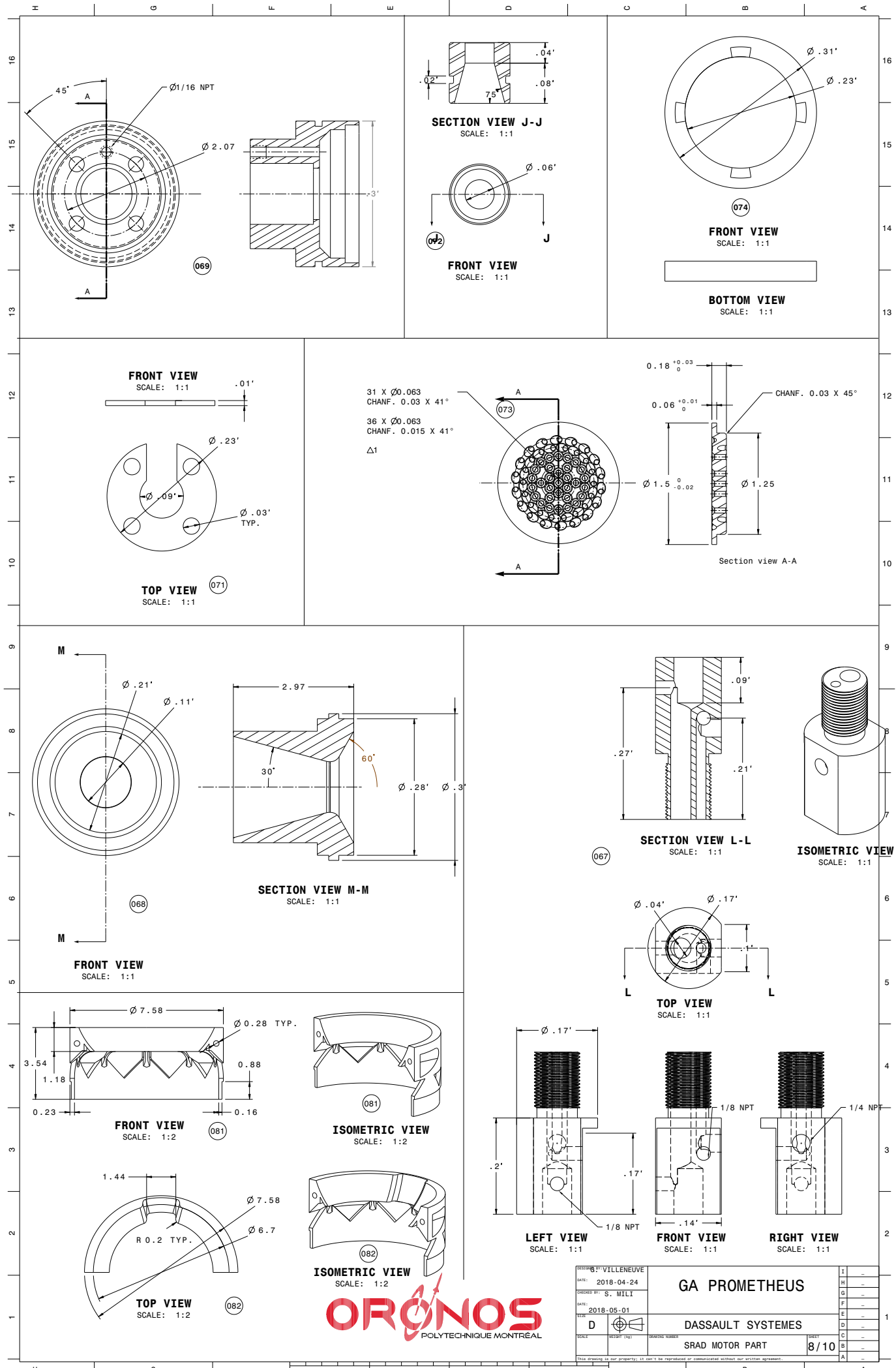
FRONT VIEW



SECTION VIEW G-C

SCALE: 1:3

DESIGNED BY: G.VILLENEUVE DATE: 2018-01-15		GA PROMETHEUS	I	-
CHECKED BY: S.MILLI DATE: 2018-03-01			H	-
SHEET 1/2	D 	DASSAULT SYSTEMES		
SCALE 1:3	001-0171 (12)	DRAWING NUMBER SECTION 3 & 4 : MOTOR BAY		7/10
		G	-	
		F	-	
		E	-	
		D	-	
		C	-	
		B	-	
		A	-	



ORONOS
POLYTECHNIQUE MONTRÉAL

RECAPITULATION OF: MA-10-00

DIFFERENT PARTS: 66

TOTAL PARTS: 343

COMPOSITE PARTS

QT	ITEM	P/N	DESCRIPTION	DEF	NOM	MATERIAL
1	001	FP-08-12	TUBE 1 : PARACHUTE BAY	ORONOS	N/A	CARBON FIBER + EPOXY
1	002	FP-08-01	TUBE 2 : AVIONIC BAY TUBE	ORONOS	N/A	CARBON FIBER + EPOXY
1	003	FP-10-02-19	TUBE 3 : MOTOR BAY SUP.	ORONOS	N/A	CARBON FIBER + EPOXY
1	004	FP-10-02-18	TUBE 4 : MOTOR BAY INF.	ORONOS	N/A	CARBON FIBER + EPOXY
1	005	FP-08-19	NOSE CONE	Madcow rocketry		FIBER GLASS + EPOXY
1	006	FP-08-21	COUPLER FOR NOSECONE	Madcow rocketry		FIBER GLASS + EPOXY
2	007	FP-08-05	COUPLER	ORONOS	N/A	CARBON FIBER + EPOXY
1	008	FP-10-02-08	COUPLER FOR MOTOR	ORONOS	N/A	CARBON FIBER + EPOXY
1	009	FP-10-02-14	COUPLER FOR MOTOR	ORONOS	N/A	CARBON FIBER + EPOXY
3	010	FP-10-02-21	FIN	ORONOS	N/A	CARBON FIBER + EPOXY

FABRICATED PARTS

QT	ITEM	P/N	DESCRIPTION	DEF	NOM	MATERIAL
1	011	FP-08-29	CENTERING BULKHEAD FOR PAYLOAD (SMALL)	ORONOS	N/A	CHERRY WOOD
1	012	FP-08-22	CENTERING BULKHEAD FOR PAYLOAD (LARGE)	ORONOS	N/A	CHERRY WOOD
3	013	FP-08-07	BULKHEAD FOR DROGUE PARACHUTE	ORONOS	N/A	CHERRY WOOD
2	014	FP-08-26	BULKHEAD FOR 5.6'' INSIDE FUSELAGE	ORONOS	N/A	CHERRY WOOD
3	015	FP-08-02	BULKHEAD FOR MAIN PARACHUTE	ORONOS	N/A	CHERRY WOOD
1	016	FP-08-28	BLOCKING RING FOR AVIONIC BAY	ORONOS	N/A	CHERRY WOOD
1	017	FP-08-22	REMOVABLE BULKHEAD FOR STRATOLOGGERS	ORONOS	N/A	CHERRY WOOD
2	018	FP-08-15A	CENTERING BULKHEAD FOR AVIONICS	ORONOS	N/A	CHERRY WOOD
1	019	FP-08-15B	CENTERING BULKHEAD FOR STRATOLOGGERS	ORONOS	N/A	CHERRY WOOD
1	020	FP-08-17	STRUCTURE PLATE FOR STRATOLOGGERS	ORONOS	N/A	CHERRY WOOD
3	021	FP-08-14	STRUCTURE PLATE FOR AVIONICS	ORONOS	N/A	CHERRY WOOD
1	022	FP-08-13	CENTERING BULKHEAD FOR AVIONICS	ORONOS	N/A	CHERRY WOOD
2	023A	FP-10-02-27	CENTERING RING FOR FUEL TANK	ORONOS	N/A	CHERRY WOOD
4	023B	FP-10-02-10	CENTERING RING FOR FUEL TANK	ORONOS	N/A	CHERRY WOOD
2	024	FP-10-02-02	CENTERING BULKHEAD FOR TOP VALVE	ORONOS	N/A	CHERRY WOOD
2	025	FP-10-02-03	CENTERING BULKHEAD FOR LOWER VALVE	ORONOS	N/A	CHERRY WOOD
2	026	FP-10-02-25	BULKHEAD FOR ENGINE (SMALL)	ORONOS	N/A	CHERRY WOOD
2	027	FP-10-02-13	RING FOR SCREWS	ORONOS	N/A	CHERRY WOOD
3	028	FP-10-02-09	BULKHEAD FOR ENGINE	ORONOS	N/A	CHERRY WOOD
3	029	FP-10-02-12	CENTERING RING FOR ENGINE	ORONOS	N/A	CHERRY WOOD
2	030	FP-10-02-23	CENTERING RING FOR FINS (TOP)	ORONOS	N/A	CHERRY WOOD
2	031	FP-10-02-22	CENTERING RING FOR FINS (MIDDLE)	ORONOS	N/A	CHERRY WOOD
2	032	FP-10-02-26	CENTERING RING FOR FINS (LOWER)	ORONOS	N/A	CHERRY WOOD
1	033	FP-10-02-24	CENTERING RING FOR FINS (BOTTOM)	ORONOS	N/A	CHERRY WOOD

STANDARD PARTS

QT	ITEM	P/N	DESCRIPTION	DEF	NOM	MATERIAL
1	034	STD-08-MC-90322A655	ROD, 1/4"-20 Thread Size, 8" Long	McMASTER	90322A655	STEEL
1	035	STD-08-MC-97088A195	TREAD ADAPTER, 1/4"-20 to 3/8"-16	McMASTER	97088A195	STEEL
1	036	STD-08-MC-90322A123	ROD, 3/8"-16 Thread Size, 2 Feet Long	McMASTER	90322A123	HIGH STRENGTH STEEL
2	037	STD-08-MC-95036A020	HEX NUT, 3/8"-16 Thread Size	McMASTER	95036A020	HIGH STRENGTH STEEL
2	038	STD-08-MC-90107A127	WASHER, 0.406" ID, 0.75" OD	McMASTER	90107A127	STEEL
3	039	STD-02-MC-95856A265	LOCKNUT, 3/8"-16 Thread Size	McMASTER	95856A265	6061 ALUMINUM
3	040	STD-02-MC-3014T471	EYEBOLT, 3/8"-16 Thread Size, 1-1/4"	McMASTER	3014T471	STEEL
3	041	STD-02-MC-90130A031	EPDM WASHER, for 3/8" Screw Size	McMASTER	90130A031	EPDM RUBBER
4	042	STD-02-MC-97763A343	SCREW, 10-32 Thread Size, 1-1/2" Long	McMASTER	97763A343	STEEL
4	043	STD-02-MC-90130A013	EPDM WASHER, for Number 12 Screw Size	McMASTER	90130A013	EPDM RUBBER
4	044	STD-02-MC-90975A015	INSERT, 10-32 Thread Size, 0.188" Long	McMASTER	90975A015	STEEL
26	045	STD-08-MC-92949A110	SCREW, 4-40 Thread Size, 1/2" Long	McMASTER	92949A110	STEEL
16	046	STD-08-MC-93181A003	HEX NUT, 4-40 Thread Size	McMASTER	93181A003	6061 ALUMINUM
11	047	STD-08-MC-92949A113	SCREW, 4-40 Thread Size, 3/4" Long	McMASTER	92949A113	STEEL
21	048	STD-02-MC-90975A002	INSERT, 4-40 Thread Size	McMASTER	90975A002	STEEL
26	049	STD-02-MC-92320A340	SPACER, 0.140" ID, 1/8" Long	McMASTER	92320A340	STEEL
12	050	STD-10-02-42-MC-91770A193	SCREW, 8-32 Thread, 7/16" Long	McMASTER	91770A193	STEEL
12	051	STD-10-02-41-MC-90973A038	INSERT, 8-32 Thread Size	McMASTER	90973A038	STEEL
4	052	STD-10-MC-95412A602	ROD, 5/16"-18 Thread Size, 10" Long	McMASTER	95412A602	STEEL
8	053	STD-10-MC-93776A441	FLANGE LOCKNUT, 5/16"-18 Thread Size	McMASTER	93776A441	STEEL
4	054	STD-10-MC-90611A400	SCREW-MOUNT NUT, 5/16"-18 Thread Size	McMASTER	90611A400	STEEL
4	055	STD-10-MC-92196A626	SCREW, 3/8"-16 Thread Size, 1.25" Long	McMASTER	92196A626	STEEL

ORONOS
POLYTECHNIQUE MONTREAL

ISSUED BY:	C.BILODEAU-B	1	-
DATE:	2018-01-15	H	-
ISSUED BY:	S.MILI	G	-
DATE:	2018-03-01	F	-
SIZE:	D	E	-
WEIGHT (kg):	(circle)	D	-
DRAWING NUMBER:	(circle)	C	-
MAKER:	(circle)	B	-
1:1	(circle)	A	-
MA-10-00		9/10	

This drawing is our property. It can't be reproduced or communicated without our written agreement.

	H	G	F	E	D	C	B	A
16								16
MOTOR PARTS								
QT	ITEM	P/N	DESCRIPTION	DEF	NOM	MATERIAL		
2	056	STD-MC-48325K282	COMPACT ACTUATED VALVE	MCMASTER	4832K282	STAINLESS STEEL		
2	057	STD-SW-SS-8-HN	NPT HEX NIPPLE 1/8"	SWAGELOK	SS-2-HN	STAINLESS STEEL		
1	058	STD-SW-SS-400-6PD-E-020	CALIBRATED OPENING	SWAGELOK	SS-400-6PD-E-020	STAINLESS STEEL		
2	059	STD-SW-SS-2-HN	NPT HEX NIPPLE 1/2"	SWAGELOK	SS-2-HN	STAINLESS STEEL		
1	060	STD-SW-SS-2-T	NPT T-FITTING, 1/2"	SWAGELOK	SS-2-T	STAINLESS STEEL		
2	061	STD-SW-SS-810-1-8	NPT-TUBE ADAPTER, 1/2"	SWAGELOK	SS-810-1-8	STAINLESS STEEL		
2	062	STD-SW-SS-NC8-TA8-PM8-12	PTFE HOSE	SWAGELOK	SS-NC8-TA8-PM8-12	PTFE, ARAMID, STAINLESS STEEL		
1	063	STD-SW-SS-8-HRCG-4	NPT FEMALE COUPLING, 1/2"	SWAGELOK	SS-8-HRCG-4	STAINLESS STEEL		
1	064	STD-SW-SS-QTM4-D-4PM	QUICK-CONNECT ADAPTER, 1/2"	SWAGELOK	SS-QTM4-D-4PM	STAINLESS STEEL		
1	065	STD-HA-XXXXXX	ACTUATED VALVE	HANBAY		STAINLESS STEEL		
1	066	STD-0M-RTD-NPT-72-E-1/8-MTP	PRESSURE TRANSDUCER	OMEGA	RTD-NPT-72-E-1/8-MTP	STAINLESS STEEL		
1	067	FP-04-01	OXIDIZER TANK ADAPTER	ORONOS	N/A	STAINLESS STEEL		
1	068	FP-04-02	NOZZLE	ORONOS	N/A	GRAPHITE		
1	069	FP-04-03	MOTOR HEAD	ORONOS	N/A	STAINLESS STEEL		
1	070	FP-04-04	MOTOR HEAD HOLDER	ORONOS	N/A	STEEL		
1	071	FP589-001	HEAD RETAINING PLATE	ORONOS	N/A	STEEL		
1	072	FP501-001	MOTOR HEAD CAP	ORONOS	N/A	STAINLESS STEEL		
1	073	FP-04-05	SWIRL INJECTOR	ORONOS	N/A	STAINLESS STEEL		
2	074	STD-CES-ROC-MOT-0003.2	PRO98 RETAINING PLATE	CESARONI	ROC-MOT-0003.2	STEEL		
1	075	N/A	PHENOLIC LINER			PHENOLIC		
4	076	N/A	FUEL GRAIN	ORONOS	N/A	PARAFFIN		
1	077	STD-CES-ROC-MOT-00000001	MOTOR CASING	CESARONI	ROC-MOT-00000001	ALUMINUM		
1	078	STD-LUX-N060	OXYDIZER TANK	LUXFER	N060	ALUMINUM		
1	079	STD-MC-48805K12	NPT ADAPTER	MCMASTER	48805K12	STAINLESS STEEL		
1	080	STD-MC-7750K24	STRAIGHT TUBE	MCMASTER	7750K24	STAINLESS STEEL		
1	081	FP-10-02-43	OXIDIZER TANK SUPPORT	ORONOS	N/A	CARBON/NYLON		
1	082	FP-10-02-44	OXIDIZER TANK SUPPORT WITH GROOVE	ORONOS	N/A	CARBON/NYLON		

ORONOS
POLYTECHNIQUE MONTREAL

DESIGNER: O'BILODEAU-B	1	-
DATE: 2018-01-15	H	-
ENCODER BY: S.MILLI	G	-
DATE: 2018-03-01	F	-
REVIEW:	D	-
APPROVAL:	C	-
MAKER:	B	-
WEIGHT (kg)	E	-
DRAWING NUMBER:	A	-
MA - 10-00	10/10	

This drawing is our property. It can't be reproduced or communicated without our written agreement.

Acknowledgments

The team would like to acknowledge the financial aid and support of Polytechnique Montreal and of our sponsors. The help of the faculty advisor, Pierre Laurendeau, is also greatly appreciated.

References

¹*Rocket Propulsion Elements* Wiley, 2010.

²*Missile Structures-Analysis and Design* Tri-State Offset Co,1967.

³*General theory of aerodynamic instability and the mechanism of flutter*, Theodorsen,1935.

⁴*The Practical Calculation of the Aerodynamic Characteristics of Slender Finned Vehicles*, Barrowman, 1967.

⁵*Aerolab*, Hans Olaf Toft, 2010.

⁶*Rasaero II*, Chuck Rogers, 2015.

⁷*Cambridge Rocketry Simulator*, Simon Box, 2008.